Supplementary Materials for

Formyl-methionine as an N-degron of a eukaryotic N-end rule pathway

Jeong-Mok Kim, Ok-Hee Seok, Shinyeong Ju, Ji-Eun Heo, Jeonghun Yeom, Da-Som Kim, Joo-Yeon Yoo, Alexander Varshavsky, Cheolju Lee*, Cheol-Sang Hwang*

*Corresponding author. Email: cshwang@postech.ac.kr (C.-S.H.); clee270@kist.re.kr (C.L.)

Published 8 November 2018 on *Science* First Release
DOI: 10.1126/science.aat0174

This PDF file includes:

Materials and methods

Miscellaneous reagents and antibodies

Cycloheximide (C7698), actinonin (A6671), trichloroacetic acid (T4885), protease inhibitor cocktail (P8215), phenylmethylsulphonyl fluoride (PMSF) (93482), iodoacetamide (I1149), endoproteinase Glu-C (P6181), antimycin A (A8674), oligomycin (O4876), potassium cyanide (60178), MOPS (M1254), sodium bisulfite (243973), zinc nitrate hexahydrate (228737) were from Sigma-Aldrich (St. Louis, MO). Chicken egg white lysozyme (LDB0308) and sodium azide (DB0613) was from Bio Basic (Markham, ON, Canada), MG-132 (474790) was from CalbioChem (San Diego, CA). Sequencing grade modified trypsin (V5111) was from Promega (Madison, WI). Phos-tag acrylamide (AAL-107) was purchased from FUJIFILM Wako Pure Chemical Corporation (Osaka, Japan). Anti-flag M2 (F1804), anti-ha (H9658), anti-c-myc (M4439), and anti-tubulin (T5168) antibodies were from Sigma-Aldrich. Anti-GST (A00865) antibody was from GenScript (Piscataway, NJ). Secondary antibodies for immunoblotting were HRP-conjugated goat anti-rabbit (170-6515, Bio-Rad, Hercules, CA) or anti-mouse (170-6516, Bio-Rad) antibodies, with detection using either Luminata Forte Western HRP substrate (WBLUF0100, Millipore, Burlington, MA) or Clarity Western ECL substrate (170-5061, Bio-Rad), according to manufacturers' instructions. Dynabeads Protein A (10001D, Thermo Fisher Scientific, Waltham, MA), Agarose-TUBE1 (UM-401, LifeSensors, Malvern, PA), and Glutathione Sepharose 4B (17-0756-05, GE Healthcare, Pittsburgh, PA) were used for immunoprecipitation and pulldown assays. $^{12}C_6$ L-Arginine:HCl (ULM-8347-H), $^{13}C_6$ L-Arginine:HCl (CLM-2265-H) and $^{13}C_6{}^{15}N_4$ L-Arginine:HCl (CNLM-539-H), for SILAC labeling of yeast proteins, were from Cambridge Isotope Laboratories (Tewksbury, MA). S^{35}-EXPRESS Met/Cys was from PerkinElmer (NEG-072, Waltham, MA).

Yeast strains, media, and genetic techniques

Table S3 list the *S. cerevisiae* strains used in this study. Construction of specific strains and transformation with DNA were done using standard techniques (*39, 40*). Media for growing *S. cerevisiae* included YPD (1% yeast extract, 2% peptone, 2% glucose), synthetic dextrose (SD) (0.17% yeast nitrogen base, 0.5% ammonium sulfate, 2% glucose), synthetic complete (SC) (SD medium plus compounds, such as, for example, specific amino acids, that were required by an auxotrophic strain), or SGal (SC medium containing 2% galactose instead of 2% glucose).

S. cerevisiae CHY3129 (*naa20Δ::natMX4 ubr1Δ::KanMX6*), CHY3186 (*ubr1Δ*::*KanMX6*), CHY3196 (*fmt1Δ::KanMX6*), CHY3174 (*psh1Δ::hphMX4*) and CHY3176 (*psh1Δ::hphMX4 naa20Δ::natMX4 ubr1Δ::KanMX6*) were constructed using PCR-mediated gene targeting and the KanMX6, hphMX4 or NatMX4 modules (*41, 42*). The E2 and E3 mutants cited in Fig. S7 were from a collection of *S. cerevisiae* deletion strains in the BY4741 genetic background (a gift from Dr. Won-Ki Huh, Seoul National University, Seoul, Korea).

Plasmids and primers

Table S4 lists the plasmids used in this study. pCH3082 expressed *E. coli* FMT from the *S. cerevisiae* P_{GAL1} promoter in the high copy (2μ-based) pRS425 vector containing T_{CYC1} terminator. The *E. coli FMT* open reading frame (ORF) was PCR-amplified from *E. coli* BL21 (DE3) genomic DNA using primers OCH2125/OCH2126 (Table S5). The resulting DNA fragment was digested with *Bam*HI/*Xho*I, and ligated into *Bam*HI/*Xho*I-cut p425GAL. To construct pCH3083, which expressed the catalytically inactive *E. coli* FMT^{R43L} mutant, PCR was used to amplify DNA from pCH3082 using primers OCH2125/OCH2127 and OCH2126/OCH2128. The

resulting DNA products were further PCR-amplified using primers OCH2125/OCH2126, digested with *Bam*HI/*Xho*I, and ligated into *Bam*HI/*Xho*I-cut p425GAL.

pCH3086 expressed MD-D2-e^K-ha-Ura3 from the P_{CUP1} promoter in the low copy (CEN-based) pRS314 vector. A pair of primers OCH3098/OCH3101 were PCR-amplified using themselves as respective templates, the DNA product was digested with *Eco*RI/*Bam*HI, and then ligated into *Eco*RI/*Bam*HI-cut pCH178.

To construct pCH3108, which coexpressed *E. coli* FMT and PDF from the bidirectional $P_{GAL1,10}$ promoter in the pRS425 vector, *E. coli PDF* ORF was first PCR-amplified from *E. coli* BL21 (DE3) genomic DNA using primers OCH3111/OCH3112. The resulting DNA fragment was digested with *Eco*RI/*Sac*I, and triply ligated (together with the *Eco*RI/*Bam*HI-cut $P_{GAL1,10}$ promoter from pCH1220) into *Sac*I/*Bam*HI-cut pCH3082. To construct pCH3109, which was otherwise identical to pCH3108 but expressed the inactive PDF^{E134A} mutant, PCR was applied to pCH3108 using primer pairs OCH3111/OCH3114 and OCH3112/OCH3113. The resulting PCR-amplified DNA fragments were again PCR-amplified using primers OCH3111/OCH3112, the product was digested with *Eco*RI/*Sac*I, and thereafter ligated into *Eco*RI/*Sac*I-cut pCH3108.

pCH3194 expressed MD-D2-e^K-ha-GST from the P_{CUP1} promoter (and T_{ADH1} terminator), and *E. coli* FMT from the P_{ADH1} promoter (and T_{CYC1} terminator) in the low copy (CEN-based) pRS314 vector. The *GST* ORF was PCR-amplified from pGEX4T-3 (Table S4) using primers OCH3193/OCH3194. The T_{ADH1} terminator DNA was PCR-amplified from *S. cerevisiae* genomic DNA using primers OCH3191/OCH2192. Two resulting PCR products were digested with *Spe*I/*Apa*I and *Apa*I/*Sac*I, respectively, and thereafter triply-ligated into *Spe*I/*Sac*I-cut pRS314, yielding an intermediate vector pCH3139. Next, P_{CUP1}-MD-D2-e^K-ha was PCR-amplified from pCH3086 using primers OCH3197/OCH3198, digested with *Sal*I/*Spe*I, and ligated into *Sal*I/*Spe*I-

cut pCH3139, thereby yielding pCH3142. *E. coli* FMT-T_{CYC1} was PCR-amplified from pCH3082 using primers OCH3247/OCH3190. The P_{ADH1} promoter sequence was PCR-amplified from *S. cerevisiae* genomic DNA using primers OCH3241/OCH3242. Finally, these PCR products were digested with *Kpn*I/*Xma*I and *Sal*I/*Xma*I respectively, and ligated into *Sal*I/*Kpn*I-cut pCH3142, thereby yielding pCH3194.

To construct pCH3558, which expressed C-terminally ha-tagged $Cse4_{ha}$ from the P_{CUP1} promoter, the *CSE4* gene was PCR-amplified from *S. cerevisiae* genomic DNA using primers OCH3549/OCH3550. The PCR product was digested with *Eco*RI/*Bam*HI and ligated into *Eco*RI/*Bam*HI-cut pCH3194. To construct pCH3567, which expressed $Cse4^{HFD}_{ha}$, two DNA fragments encoding Cse4 immediately before and immediately after the CATD region were amplified from pCH3558, using the primer pairs OCH3549/OCH3589 and OCH3590/OCH3550. In addition, DNA encoding the histone H3 HFD segment was PCR-amplified from *S. cerevisiae* genomic DNA using primers OCH3587/OCH3588. DNA encoding $Cse4^{HFD}_{ha}$ was then amplified from a mixture of the three above PCR-produced DNA fragments, using the method of overlapping extension PCR, in which partially formed duplex DNAs contained truncated *CSE4* and *H3 HFD* fragments as well as 3' overhangs that enabled yet another PCR, with the primers OCH3549/OCH3550. The resulting PCR product was digested with *Eco*RI/*Bam*HI and ligated into *Eco*RI/*Bam*HI-cut pCH3194.

Details of cloning procedures for other plasmids listed in Table S4 are available upon request. All final plasmids were verified by DNA sequencing.

Cycloheximide (CHX)-chase degradation assays

CHX chases were carried out essentially as previously described (*12*). *S. cerevisiae* cells were grown to A_{600} of 0.8-1.0 at 30℃ in selective media appropriate for a plasmid(s) carried by a given

strain, and were treated with CHX at the final concentration of 0.1 mg/ml. Cell samples (equivalent to 1 ml of cell suspension at A_{600} of 1) were harvested at indicated times by centrifugation for 1 min at 11,200*g*. For the CHX-chases with stationary-phase *S. cerevisiae*, cells were grown for 48 hr (to A_{600} of ~4.0) at 30°C in SC medium with 5 μM $CuSO_4$ and appropriate metabolic markers for a plasmid(s) carried by a given strain. Stationary-phase cells were treated with CHX at the final concentration of 0.5 mg/ml. Cell samples (equivalent to 1 ml of cell suspension at A_{600} of 2) were harvested at indicated times by centrifugation for 1 min at 11,200*g*. CHX-chases with $Rps22a_{ha}$ and $Pgd1_{ha}$ in wild-type *S. cerevisiae* without ectopic expression of either *E. coli* FMT or ScFmt1 were performed as described above except that plates with yeast were kept at 4℃ for 14 days before inoculation into an SC-based liquid medium and growth to stationary phase as described above. The samples were resuspended in 1 ml of 0.2 M NaOH, and thereafter incubated for 20 min on ice. After centrifugation for 1 min at 11,200*g*, the pelleted cells were resuspended in 50 μl of HU buffer (8 M urea, 5% SDS, 1 mM Na-EDTA, 0.1 M dithiothreitol (DTT), 0.005% bromophenol blue, 0.2 M Tris-HCl, pH 6.8) containing 1x protease inhibitor cocktail (Sigma-Aldrich), and heated for 10 min at 70℃. After centrifugation for 5 min at 11,200*g*, 10 μl of supernatant was subjected to SDS-12%, 10% or 4-20% Tris-glycine PAGE, followed by immunoblotting with either anti-MD-$D2^{fM}$ (1:1,000), or anti-$Cse4^{fMet}$ (1:1,000), or anti-ha (1:2,000), or anti-flag (1: 2000), or anti-GST (1:2,000), or anti-tubulin (1:2,000) antibody. Quantifications of chase data were performed using the ImageJ software (http://rsb.info.nih.gov/ij/index.html).

In vivo ^{35}S-Met/Cys labeling assay

S. cerevisiae cells were grown at 30℃ to A_{600} of 0.8-1.0 in 10 ml of SD medium (with amino acids required for growth of a strain), and were harvested by centrifugation for 1 min at 11,200*g*. The pelleted cells were washed in 0.8 ml of SD media (without L-Met and L-Cys), and resuspended in 0.4 ml of the same media. After incubation at 30℃ for 10 min, cell suspensions were supplemented with L-Met (at 4 mM), L-Cys (at 2 mM), and 0.16 mCi of ^{35}S-EXPRESS Met/Cys (Perkin-Elmer). Samples (0.1 ml) were taken at indicated time points, followed by preparation of extracts as described above for CHX-chase assays. Appropriately (and uniformly, about 50-fold) diluted 10-μl samples were subjected to SDS-4-20% Tris-glycine PAGE, followed by Coomassie staining and/or ^{35}S-autoradiography.

Northern RNA analyses

Total RNAs were isolated from *S. cerevisiae* using RiboPure-Yeast Kit (AM1926, Thermo Fisher Scientific) and Northerns were performed using DIG Northern Starter Kit (12039672910, Roche). 1 μg of total RNA was separated by formaldehyde-agarose gel electrophoresis, and transferred to a positively charged nylon membrane (RPN303B, GE Healthcare), using Semi-Dry Transfer Cell (VE-386, Tanon, Shanghai, China). Transferred RNAs were UV-crosslinked to membrane, pre-hybridized using DIG Easy Hyb Granules (11796895001, Roche) for 1 hr at 68℃, and thereafter hybridized overnight at 68℃ in the presence of *MD-D2-e^K-ha-GST* or *ACT1* RNA probes. The synthesis of digoxigenin (DIG)-labeled *MD-D2-eK-ha-GST* and *ACT1* RNAs was carried out by in vitro transcription of *Spe*I-cut pCH3219 (or a PCR-amplified *ACT1* cDNA) using T7 RNA polymerase and a mixture of DIG-11-UTP and unlabeled dNTPs. After hybridization with RNA probes, a membrane was washed twice at 25℃ for 5 min with 2xSSC, 0.1% SDS, and thereafter washed twice at 68℃ for 15 min with 0.1% SDS, 0.1xSSC. Hybridization patterns were visualized

using anti-digoxigenin antibody conjugated with alkaline phosphatase and the CDP-*STAR* ready-to use substrate (12041677001, Roche).

Purification and mass spectrometric analyses of Nt-formylated fMD-D2-GST

To produce Nt-formylated fMD-D2-GST, we used *E. coli* AG100A [*acrAB⊿* BL21(DE3] lacking the efflux pump AcrAB (*43*). 10 ml of overnight culture of AG100A carrying pCH2182 (Table S4) were inoculated into 1 l of Lysogeny Broth (LB) medium containing ampicillin (final concentration of 0.1 mg/ml), followed by growth at 37℃ to A_{600} of ~0.7. Expression of MD-D2-GST was induced by incubating *E. coli* with 1 mM IPTG at 30℃ for 4 hr. To produce Nt-formylated fMD-D2-GST, the deformylase inhibitor actinonin (at the final concentration of 2 μg/ml) was added to a culture together with IPTG. Cells were harvested by centrifugation for 15 min at 2,000*g* and frozen at -80℃. Cell pellets were thawed and resuspended in STE buffer (0.1 M NaCl, 1 mM EDTA, 10 mM Tris-HCl, pH 8.0) containing 1 mM DTT, 1 mM PMSF, and 1mg/ml of chicken egg white lysozyme. Resuspended cells were incubated on ice for 20 min, and thereafter disrupted by sonication (VCX-500, SONICS, Newtown, CT), 12 times for 2 sec each, at 8 sec intervals with 40% amplitude. After centrifugation at 11,200*g* for 30 min, a supernatant was incubated with 1 ml of Glutathione Sepharose 4B (GE Healthcare) at 4°C for 2 hr. After extensive washing with 20 ml of STE buffer, the bound MD-D2-GST was eluted with 6 ml of STE buffer containing 10 mM reduced glutathione, followed by overnight dialysis against storage buffer (10% glycerol, 0.15 M NaCl, 1mM DTT, 50 mM Tris-HCl, pH 8.0). To determine the formylation state of purified fMD-D2-GST its 2-μg sample was denatured, reduced, digested and then analyzed by nanoflow liquid chromatography-tandem mass spectrometry (LC-MS/MS) using the LTQ Orbitrap Velos (Thermo Fisher Scientific) hybrid mass spectrometer at the Pohang Center

for Evaluation of Biomaterials (Pohang, Korea), as previously described (*13*). The Nt-formylation site was assigned using MaxQuant software package (*44*) and through manual inspections of MS/MS spectra.

Preparation of proteins using SILAC

S. cerevisiae CHY153 cells (*arg4Δ::kanMX6* in JD52) carrying either p425GAL (vector) or pCH3082 (expressing *Ec*FMT) were grown at 30℃ to A_{600} of ~1.0 in 300 ml of SGal medium with either light $^{12}C_6$ L-arginine (at 20 mg/l) or heavy $^{13}C_6$-arginine (at 20 mg/l). Equal amounts of cells (equivalent to A_{600} of 300) from each culture were mixed and centrifuged at 4℃ for 10 min at 2,000*g*. After washing two times with cold PBS (phosphate-buffered saline), the pelleted cells were resuspended in 6 ml of lysis buffer (6 M guanidine-HCl, 0.5 % Nonidet P-40 (NP40), 10 mM DTT, 50 mM HEPES, pH 8.0), and disrupted by bead beating using Mini-Beadbeater-24 (BioSpec Products, Bartlesville, OK) (4 times for 15 sec each at 1 min intervals, with cooling on ice). After centrifugation at 4℃ for 15 min at 11,200*g*, 6 ml of the resulting supernatant was precipitated on ice for 10 min with 0.6 ml of 100% CCl_3COOH, followed by centrifugation at 4℃ for 15 min at 11,200g, and two washed of the pellet with 0.5 ml of cold acetone.

For analyses of stationary-phase cells, *S. cerevisiae* CHY3188 (*arg4Δ::kanMX6* in JD53) or CHY3189 (*arg4Δ::kanMX6 psh1Δ::hphMX4* in JD53) were independently inoculated and grown in triplicate for 48 hr (to A_{600} of ~4.0) at 30℃ in 50 ml of SC medium with either light $^{12}C_6$ L-arginine (at 50 mg/l) or heavy $^{13}C_6{}^{15}N_4$-arginine (at 50 mg/l). Equal amounts of cells (equivalent to A_{600} of 200) from each culture of a set of replicates were mixed and centrifuged at 4℃ for 10 min at 2,000*g*. This procedure was repeated identically for other sets of replicates, resulting in independent triplicates of mixed cell cultures. After washing two times with cold PBS (phosphate-

buffered saline), cell pellets were resuspended in lysis buffer (6 M guanidine-HCl, 0.2 M HEPES, pH 8) containing 1x protease inhibitor cocktail (Sigma-Aldrich), followed by disruption using Mini-Beadbeater-24 (BioSpec Products). The final concentration of total protein in each sample was ~1 mg/ml.

Enrichment for N-terminal peptides and cLC-MS/MS analyses

5 mg of total protein (see above) in 5 ml of sample buffer (6 M guanidine-HCl, 0.1 M HEPES, pH 8.5) from extracts of *S. cerevisiae* that expressed either vector alone or *Ec*FMT (see the main text) were processed to enrich for Nt-peptides as previously described (*45*). The proteins were digested by trypsin at 1:50 enzyme/protein ratio for 16 hr at 37°C, and the enriched Nt-peptides were pre-fractionated into six fractions by manual basic reversed phase liquid chromatography (bRPLC) method (*45*). Peptides were dried in vacuum and kept at -80℃ until use. For cLC-MS/MS analyses of wild-type and *Ec*FMT-expressing *S. cerevisiae*, dried peptide samples were redissolved in 0.4% acetic acid, and a sample containing ~1 μg of peptides was injected from a cooled (10°C) autosampler into a reversed-phase Magic C18aq (Michrom BioResources, Auburn, CA) column (15 cm × 75 μm, packed in-house) on an Eksigent nanoLC-ultra 1D plus system (Eksigent Technologies, Dublin, CA) at a flow rate of 300 nl/min. Prior to use, the column was equilibrated with 90% buffer A (0.1% formic acid in water) and 10% buffer B (0.1% formic acid in acetonitrile). Peptides were eluted with a linear gradient from 10% to 50% buffer B over 90 min and 50% to 80% buffer B over 5 min, followed by wash with 0.1% formic acid in 70% acetonitrile for 10 min, and an aqueous re-equilibration at a flow rate of 300 nl/min, with a total run time of 120 min. The HPLC system was coupled to a Q-Exactive mass spectrometer (Thermo Fisher Scientific, Waltham, MA) operated in a data-dependent acquisition (DDA) mode. Survey full-scan MS spectra (m/z

300–1800) were acquired with resolution of 70,000. Source ionization parameters were as follow: spray voltage, 1.9 kV; capillary temperature, 275°C; and s-lens level, 44.0. The MS/MS spectra of 12 most intense ions from the MS1 scan with a charge state 1 to 5 were acquired as follows: resolution, 17,500; automatic gain control (AGC) target, 1E5; isolation width, 2.0 m/z; normalized collision energy, 27%; dynamic exclusion duration, 40 s; and ion selection threshold, 4.00E+03 counts.

To enrich for Nt-peptides with extracts of stationary-phase *S. cerevisiae*, similar procedures were employed. Specifically, protein digestion was performed with trypsin, and free amino groups of resulting peptides were derivatized with D_6-acetic anhydride rather than propionic acid. The enriched Nt-peptides were pre-fractionated by bRPLC using an XBridge Peptide BEH C18 column (250 mm × 4.6 mm, 3.5 µm, 130 Å ; Agilent) on the Agilent 1290 UHPLC system, at the flow rate of 0.5 ml/min. The solvent used were 10 mM ammonium formate pH 10.0 (solvent A) and 10 mM ammonium formate with 90% (v/v) acetonitrile (pH 10) (solvent B). The gradient started from 0% of solvent B, and was increased to 5% B in 10 min, to 40% B in 38.5 min, to 70% B in 14 min, and held at 70% B for 10 min, decreasing to 5% B over next 10 min. Fractions were collected every 0.8 min from 10 min to 77.2 min and were pooled into 12 fractions by taking every 12th fraction. Specifically, fraction 1, 13, 25, 37, 49, 61, and 73 were combined to yield fraction I; fractions 2, 14, 26, 38, 50, 62, and 74 were combined to yield fraction II, and so forth, resulting in fractions I-XII. Pooled fractions were dried using vacuum concentrator. Thereafter, EASY-Spray Columns (15 cm × 75 µm, Thermo Fischer Scientific) were used for cLC-MS/MS, to separate peptides in each of the pooled 12 fractions. The solvents used were 0.1% formic acid in water (solvent C) 0.1% formic acid in acetonitrile (solvent D). After injection of the sample into the column equilibrated with 98% solvent C and 2% solvent D, peptides were eluted with the following

gradient: 2% solvent D for 5 min, followed by 2% to 30% solvent D over 110 min, 30% to 70% solvent D for 3 min, and holding 70% solvent D for 12 min. The above mass spectrometer was used, with surveys of full MS scans (m/z 400-1800). AGC target of MS/MS spectrum, 5E4; dynamic exclusion duration, 30 s; and ion selection threshold, 4.2E+03 counts.

Proteome database searches and SILAC-based quantification

RAW-files directly from the Q-Exactive mass spectrometer were converted into mgf-files using the Proteome Discoverer version 1.4 software (Thermo Fisher Scientific) with default options. All spectra were first matched to peptide sequences in the UniProtKB yeast database (release 2013. 10) using MS-GF+ (v10072) and Comet (2016.01 rev. 2) search engines. The search engine settings were as follows: 1 as the number of tolerable termini; 15 ppm for MS1 tolerance; 0, 2 as IsotopeErrorRanges; allow to decoy database search; variable modifications: oxidation of methionine (+15.9949 Da), acetyl (+42.0106 Da), or propionylation (+56.026215 Da), or formylation (+27.9949 Da) of the N-terminus, SILAC labeling of arginine (+6.020129 Da); fixed modification: methylthio of cysteine (+45.9877 Da) and propionylation (+56.026215 Da) of lysine. Search outputs from MS-GF+ and Comet were conveyed to Percolator for estimation of PSM (peptide spectrum match) level FDR (false discovery rate) of peptide identification. FDR was set to 1% at the PSM level.

For SILAC-based MS/MS experiments from stationary-phase yeast cells, we converted raw-files into mzXML files using ProteoWizard software (v3.0.18137) with peak centroiding option (from MS1 to MS2). The converted mzXML files were searched with MS-GF+ (v2018.04.09) and UniProtKB yeast database (release 2018. 1). The search engine settings were as follows: 1 as the number of tolerable termini; 0, 2 as IsotopeErrowRanges; allowed decoy database searches;

variable modifications: acetyl to peptide N-term., D_3-acetyl (+45.029395 Da) to peptide N-term., formyl to protein N-term., oxidation of methionine, and SILAC-heavy of arginine (+10.008269 Da) to arginine; fixed modification: carbamidomethylation of cysteine, D_3-acetylation of lysine. Search outputs containing peptide identification results and estimated PSM-level FDR were directly conveyed to Microsoft EXCEL using MS-GF+ integrated export tool. We employed PSMs only if they were less than 1% FDR of PSM level.

Production and purification of anti-MD-D2^{fM} and anti-Cse4^{fM} antibodies

The two peptide antigens were the Nt-formylated synthetic peptide fMDIAIGTYQEKC and its unformylated counterpart MDIAIGTYQEKC. Except for Asp at position 2 and C-terminal Cys (used for conjugation of a peptide to the keyhole limpet hemocyanin carrier), the sequence of these peptides was identical to the sequence of 11 Nt-residues of the *C. reinhardtii* chloroplast D2 protein (*7*). Rabbit polyclonal antisera to the two peptides were produced by AbFrontier (Seoul, Korea). Antibodies specific for fMDIAIGTYQEK were "negatively" selected from antiserum by passing 5 ml of clarified antiserum through 1 ml of glutathione-Sepharose (GE Healthcare) that had been incubated overnight at 4℃ with and 4.8 mg of the purified (see above) unformylated MD-D2-GST. To further increase the specificity of antibody for Nt-formylated fMD-D2-based fusions, the above flow-through fraction was incubated at 4℃ with 1 ml of cyanogen bromide (CNBr)-activated Sepharose (C9142 Sigma-Aldrich) that had been conjugated with 30 mg of proteins from a whole-cell wild-type *S. cerevisiae*. The unbound IgG was concentrated by Protein A-Sepharose affinity chromatography (Amicogen, Seoul, Korea), yielding the preparation of antibody denoted as anti-MD-D2^{fM}.

To raise antibody specific for Nt-formylated *S. cerevisiae* Cse4, two synthetic peptides were produced, the Nt-formylated fMSSKQQWVSSAGSC and its unformylated counterpart MSSKQQWVSSAGSC. Except for Gly-Ser (linker) followed by C-terminal Cys (used for conjugation to keyhole limpet hemocyanin), these peptides were identical to the sequence of 11 Nt-residues of yeast Cse4. Nt-formylated fMet-Cse4$^{2-16}$-GST, bearing the 16 Nt-residues of Cse4 and its unformylated Met-Cse4$^{2-16}$-GST counterpart were expressed in *E. coli* in the presence vs. absence of actinonin, and were purified as described above for fMD-D2-GST and MD-D2-GST.

Rabbit polyclonal antisera to the two Cse4-derived peptides were produced by AbClon (Seoul, Korea). 175 μg of Nt-formylated fMet-Cse4$^{2-16}$-GST and 275 μg of unformylated Met-Cse4$^{2-16}$-GST were conjugated to 0.8-ml samples of CNBr-activated Sepharose. Antibodies specific for Nt-formylated fMSSKQQWVSSA were then "negatively" selected from antiserum (5 ml) by incubating it with 0.8 ml of Sepharose conjugated with unformylated Met-Cse4$^{2-16}$-GST overnight at 4℃. The unbound (flow-through) fraction was incubated with 0.8 ml of Sepharose conjugated to Nt-formylated fMet-Cse4$^{2-16}$-GST overnight at 4℃. The resulting suspension was washed 5 times with 10 ml PBS, and the bound antibodies were eluted with 3 ml of 0.1 M glycine-HCl (pH 3.3). The eluted fraction was neutralized to neutral pH with 1 M Tris (pH 8.0) and thereafter concentrated by Protein A-Sepharose chromatography (Amicogen), yielding the antibody termed anti-Cse4^{fM} (fig. S4, C and D). Anti-MD-D2^{fM} and anti-Cse4^{fM} antibodies (at 1:1,000 dilution) were incubated with immunoblotting membranes for 16 hr at 4℃ in PBST (PBS containing 0.5% Tween-20). The bound antibodies were detected using a goat anti-rabbit antibody (at 1:5,000 dilution) conjugated to horse radish peroxidase (Bio-Rad).

GST-pulldown assays

GST-pulldown assays were performed with *S. cerevisiae* JD53 carrying the plasmid pCH3282 that expressed C-terminally flag-tagged $Psh1_f$. Yeast cells were grown at 30℃ to A_{600} of ~3.0 in 1 l of SC medium with amino acids required for growth. Cells were harvested by centrifugation at 2,000*g* for 15 min and frozen in -80℃. Cell pellets were thawed and resuspended in lysis buffer (10% glycerol, 1% NP40, 0.2 M KCl, 1 mM DTT, 50 mM HEPES, pH 7.5) containing 1x protease inhibitor cocktail (Sigma-Aldrich). Cells were disrupted using Mini-Beadbeater-24 (BioSpec Products). 1 mg of total protein (~10 mg/ml) of a clarified cell extract was incubated at 4℃ overnight with 50 μg of purified Nt-formylated fMD-D2-GST or unformylated MD-D2-GST in the binding buffer (10% glycerol, 0.5 M NaCl, 1 % NP40, 1 mM EDTA, 50 mM Tris-HCl, pH 8.0). 50 μl of glutathione-Sepharose 4B (50% slurry) was then added to each sample, and suspensions were further incubated, with rocking, at 4℃ for 4 hr. Glutathione-Sepharose beads were then washed 3 times with 0.5 ml of the binding buffer, and the bound proteins were eluted by incubating samples with 15 μl of 2xSDS-sample buffer at 70℃ for 5 min. The resulting samples were clarified by centrifugation at 11,200*g* for 1 min, and the supernatants were subjected to SDS-12% Tris-glycine PAGE, followed by immunoblotting with anti-MD-$D2^{fM}$, anti-flag, and anti-GST antibodies.

In vivo polyubiquitylation assays

Extracts from *S. cerevisiae* strains CHY3129 and CHY3176 (carrying pCH3219, pCH3220 and pCH3323) were prepared as described above in the section about GST-pulldown assays, except that the lysis buffer was different (10% glycerol, 1% NP40, 0.15 M NaCl, 5 mM N-ethylmaleimide (NEM), 2 mM EDTA, 1 mM DTT, 50 mM Tris-HCl, pH 7.5). 3 mg of total protein (~10 mg/ml) of a clarified cell extract were incubated at 4℃ for 16 hr with 10 μl of TUBE1-agarose beads (50%

slurry) (LifeSensors). The beads were washed 3 times with 0.5 ml of TBS-T buffer (0.1% Tween-200, 15 M NaCl, 20 mM Tris-HCl, pH 8.0), and the TUBE1-agarose-bound proteins were eluted by incubating samples with 15 μl of 2xSDS-sample buffer at 70℃ for 10 min. The resulting samples were clarified by centrifugation at 11,200*g* for 5 min, and the supernatants were subjected to subjected to SDS-Tris/gycine-12% PAGE followed by immunoblotting with anti-GST antibody.

Immunoprecipitation of Nt-formylated fMD-D2-GST

S. cerevisiae strains CHY3006 and CHY3196 carrying pCH2200 were grown at 30℃ for 24 hr (A_{600} of ~2.5) or 72 hr (A_{600} of ~4.0) in 100 ml of SC medium with required amino acids. Cell extracts were prepared as described in the section about GST-pulldown assays. 1 mg of total protein of a clarified cell extract (~10 mg/ml) and 1 μl of anti-MD-D2^{fM} antibody were incubated at 4℃ for 16 hr in the binding buffer (10% glycerol, 1% NP40, 0.5 M NaCl, 1mM EDTA, 50 mM Tris-HCl, pH 8.0). 5 μl of Dynabeads-Protein A (10001D, Thermo Fisher Scientific) were then added at 4℃ for 2 hr. The beads were washed 3 times with 0.5 ml of the binding buffer, and the bound proteins were eluted by incubating samples with 50 μl of 1xSDS-sample buffer at 70℃ for 10 min. The resulting samples were clarified by centrifugation at 11,200*g* for 5 min, and 8 μl of the supernatants were subjected to subjected to SDS-12% Tis-glycine PAGE, followed by immunoblotting with anti-GST antibody.

Phos-tag-based electrophoretic mobility shift assay

In the Phos-tag™-based mobility-shift detection of phosphorylated proteins (Wako Chemical Corporation), a protein sample that contains phosphorylated proteins is subjected to a version of SDS-PAGE in which a polyacrylamide gel contains a covalently conjugated Phos-tag compound

that specifically and selectively binds to phosphate groups of phosphoproteins that migrate through the gel. As a result, while a non-phosphorylated (or less extensively phosphorylated) form of a given protein migrates through the gel, the electrophoretic mobility of its (more) phosphorylated form is decreased, resulting in a slower migrating band. This gel-shift assay makes it possible to fractionate a specific protein (with its detection using, e.g., immunoblotting) as a function of its phosphorylation state.

S. cerevisiae strains JD53 and CHY3200 (*gcn2Δ*) carrying the pCH3417 plasmid (which coexpressed *Sc*Fmt1$_{myc}$ and MD-D2-GST) were inoculated (at A_{600} of 0.2) into 6 ml of SC(-Trp) media supplemented with either 20 μg/ml or 2 μg/ml of L-histidine. Cells were grown for 24 hrs at 30℃ on a test tube rotator. Protein samples were prepared thereafter as described in the section about CHX-chase assays. After clarifying 50-μl protein samples in HU buffer by centrifugation at 11,200*g* for 5 min, 3-μl samples of supernatants were loaded onto a 10% polyacrylamide gel containing with 25 μM Phos-tag acrylamide (Wako Chemical Corporation) and 50 μM zinc nitrate hexahydrate ($Zn(NO_3)_2•6H_2O$).

Phos-tag analyses were performed according to manufacturer's instructions, with slight modifications. Briefly, Phos-tag gel electrophoresis was run on ice, using ice-cold running buffer (0.1 M Tris, 0.1 M MOPS, 0.1% SDS, 5 mM Na-bisulfite, pH 7.8) with step-wise changes of voltage, from 60V, 70V, and 80V to 100V, as the Bromophenol Blue (indicator dye) migrated, initially, to the stacking gel, and to the one-third, one half and the end of resolving gel, respectively. To chelate Zn^{2+} after electrophoresis, Phos-tag gels were washed three times for 10 min with ice-cold EDTA-transfer buffer (10 mM EDTA, 25 mM Tris, 192 mM glycine, 20% methanol). Thereafter, to remove excess EDTA, the gels were washed once for 10 min in ice-cold EDTA-free transfer buffer. Proteins in the resulting Phos-tag gel were electroblotted onto PVDF membrane in

SDS-transfer buffer (0.05% SDS, 25 mM Tris, 192 mM glycine, 20% methanol) with constant current (0.1 A) for 16 hr at 4℃, and then at 0.2 A for 3 hr at 4℃. The transferred $Fmt1_{myc}$ was detected on PVDF membrane using anti-c-myc antibody (1:2,000).

Fluorescence microscopy of EGFP-tagged proteins

S. cerevisiae JD53 carrying either the pCH2194 plasmid, which expressed the C-terminally 3xEGFP-tagged *Sc*Fmt1 (*Sc*Fmt1-$EGFP_3$), or the pCH2195 plasmid, which expressed *Sc*$Fmt1^{\Delta 1-26}$-$EGFP_3$, were grown at 30℃ for 6 hr, to A_{600} of ~0.8, or for 72 hr, to A_{600} of ~4.0, in 5 ml of SC medium with required amino acids. To compare localization of other (non-*Sc*Fmc1) nuclear DNA-encoded mitochondrial-matrix proteins with that of *Sc*Fmt1, *S. cerevisiae* JD53 cells carrying either pCH3423 (Ifm1-EGFP), or pCH3425 (Sod2-EGFP), or pCH3426 (Cit1-EGFP) were grown as described above. In all of these assays, *S. cerevisiae* also carried the pCH3383 plasmid, which expressed mito-mCherry, a fluorescent mitochondrial marker (*46*). Cells (equivalent to 1 ml of cell suspension at A_{600} of ~2) were collected at indicated times by centrifugation for 1 min at 11,200*g*. Cell pellets were resuspended in 0.1 ml of fixation solution (4% formaldehyde (from paraformaldehyde), 3.4% sucrose, 0.1 M K-phosphate, pH 7.5) and incubated at room temperature for 15 min. The resulting cell suspensions were centrifuged for 1 min at 11,200*g*, washed once with 1 ml of resuspension buffer (1.2 M sorbitol, 0.1 M potassium phosphate, pH 7.5), and resuspended in 0.1 ml of the same buffer. 2-µl samples of cell suspensions were examined for EGFP or mCherry fluorescence patterns using Zeiss Axio Scope-A1, and Adobe Photoshop.

Quantification criteria for relative levels of the cytosol-localized *Sc*Fmt1-$EGFP_3$ in wild-type cells versus *gcn2Δ* cells: we defined *Sc*Fmt1-$EGFP_3$ as being localized largely in the cytosol if the fluorescence occupied, evenly, more than 80% of the entire area of a yeast cell, i.e.,

identically to "model" cytosolic species of *Sc*Fmt1$^{\Delta 1\text{-}26}$-EGFP$_3$ which lacked the mitochondrial presequence and remained constitutively cytosolic. Quantification data in Fig. 4D were collected with ~300 cells of each yeast strain, in three independent experiments.

Cell growth assays

To examine effects of Nt-formylation in the yeast cytosol on cell growth, JD53 (wild-type) and CHY3174 (*psh1Δ*) *S. cerevisiae* carrying pCH3323 (wild-type *Ec*FMT) or pCH3324 (inactive *Ec*FMT^{R43L} mutant) in the presence of either pCH5109 (wild-type *Ec*PDF) or pCH5110 (inactive *Ec*PDF^{E134A} mutant), were grown to A_{600} of ~1 at 30℃ in 5 ml of SC media with required amino acids. *S. cerevisiae* cultures were initiated at A_{600} of ~0.05 in 0.2 ml samples of SC media with required amino acids in a 96-well microplate (32096, SPL, Pochen, Korea). Thus prepared plates were incubated at 30℃ with double orbital shaking (282 rpm) for 30 hr, with measurements of A_{600} at 10-min intervals using Epoch 2 microplate spectrophotometer (BioTek, Winooski, VT). To examine colony growth on solid media, *S. cerevisiae* JD53 and CHY3174 carrying p425GAL (vector alone) or pCH3082 (wild-type *Ec*FMT) were grown to A_{600} of ~1 at 30℃ in SC(-Leu) medium. Each culture (equivalent to 1 ml of cell suspension at A_{600} of 1) was washed twice, serially diluted 5-fold in distilled water, and spread onto SC(-Leu) and SGal(-Leu) plates containing, respectively, 2% glucose and 2% galactose. Plates were incubated for 2 or 4 days at 30°C.

To address the influence of *Ec*PDF expression on cell growth, wild-type *S. cerevisiae* BY4741 and their specific mutants (*cox5aΔ*, *atp11Δ*, *coq5Δ*) carrying pCH3101 (vector), pCH3397 (expressing wild-type *Ec*PDF) or pCH3398 (expressing the catalytically inactive *Ec*PDF^{E134A} mutant), were grown to A_{600} of ~1 at 30℃ in SC(-Leu) medium. Equal volumes of

cultures were harvested by centrifugation for 1 min at 11,200*g*, and washed once with 1 ml of distilled water. Each pelleted cell was resuspended with 1ml of distilled water, and equal volumes of 5-fold serially diluted cells were spotted on SGal(-Leu) plates containing 2% galactose. The plates were incubated at 30℃ for 2-3 days.

The Nt-formylation-relevant effect of a prolonged (~14 days) pre-incubation of yeast at 4°C (Fig. 5 and fig. S12) was discovered accidentally, and became a part of our tests. *S. cerevisiae* JD53 carrying pCH3101 (vector), pCH3397 (expressing wild-type *Ec*PDF) or pCH3398 (expressing the catalytically inactive *Ec*PDF^{E134A} mutant) were kept on SC plates at 4°C for 0, 7 or 14 days. Each sample (equivalent to 1 ml of cell suspension at A_{600} of 1) was harvested from a plate, washed once with 1 ml of distilled water, and resuspended in 1 ml of water. Cell suspensions were diluted with SC(-Leu) media with required amino acids to A_{600} of ~0.05 in 0.2 ml samples of SC(-Leu) media in wells of a 96-well microplate, the microplate was placed on a rotary shaker and the growth of each cell culture (at 30°C) was followed using Epoch2 microplate spectrophotometer as described above.

In other assays that involved low-temperature pre-incubations, *S. cerevisiae* JD53 carrying pCH3101 (vector), pCH3397 (expressing wild-type *Ec*PDF) or pCH3398 (expressing the inactive *Ec*PDF^{E134A} mutant) were kept on plates for 14 days at 4℃, and thereafter inoculated into SC(-Leu) media as described above , followed by incubation on a test tube rotator at 30℃ for 16 hr. Equal amounts of cultures (equivalent to 1 ml of A_{600} of ~2.0) were harvested by centrifugation, washed once with 1 ml of distilled water, serially diluted 5-fold in distilled water, and thereafter spotted onto SGal(-Leu) plates either with or without the following stressors: Na-azide (NaN_3) (20 μM), antimycin A (20 nM), oligomycin (5 μM), potassium K-cyanide (KCN) (1 mM). The plates were incubated at 30℃ for 2-3 days.

To verify whether the *Sc*Fmt1-EGFP$_3$ fusion was functionally active as a formyltransferase, *S. cerevisiae* W303-1A (wild-type) and its derivative CHY909 (*fmt1Δ*) carrying pRS316 (vector) or pCH2194 (expressing *Sc*Fmt1-EGFP**3**) were grown to A_{600} of ~1 at 30℃ in SC(-Ura) medium. Equal volumes of cultures were harvested, washed once and resuspended with 1ml of distilled water, followed by 5-fold serially dilution with water. Equal volumes of diluted cells were spotted on SC(-Ura) and SGly(-Ura) plates containing, respectively, 2% glucose and 2% glycerol (*47*). The plates were incubated at 30℃ for 2-3 days.

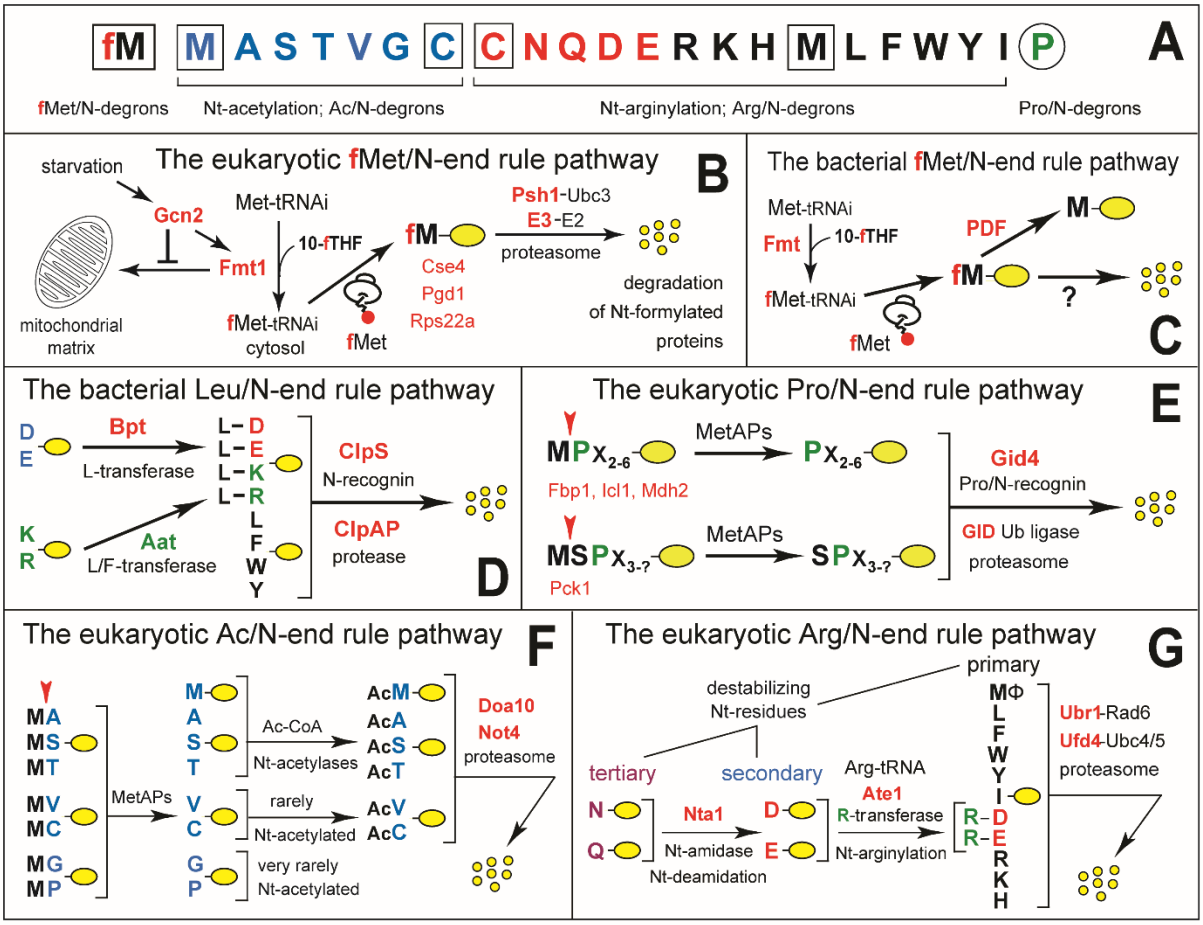

Fig. S1. Eukaryotic and prokaryotic N-end rule pathways. (**A**) N-terminal (Nt) residues are indicated by single-letter abbreviations. Twenty amino acids of the genetic code are arranged to delineate specific N-end rule pathways. Nt-Met is cited thrice, because it can be recognized by the Ac/N-end rule pathway (as Nt-acetylated Met), by the Arg/N-end rule pathway (as the unacetylated N-terminal Met), and by the fMet/N-end rule pathway (as Nt-formylated Met). Nt-Cys is cited twice, because it can be recognized by the Ac/N-end rule pathway (as Nt-acetylated Cys) and by the Arg/N-end rule pathway (as an oxidized, Nt-arginylatable Nt-Cys sulfinate or sulfonate, formed in multicellular eukaryotes but apparently not in *S. cerevisiae*, at least not in the absence of stress) (*9*, *26*). (**B**) The eukaryotic (*S. cerevisiae*) fMet/N-end rule pathway discovered in the present work (see the main text). 10-fTHF, 10-formyltetrahydrofolate. (**C**) The bacterial (*E. coli*) fMet/N-end rule pathway (*7*). (**D**) The bacterial (*Vibrio vulnificus*) Leu/N-end rule pathway (*10*, *21*). (**E**) The eukaryotic (*S. cerevisiae*) Pro/N-end rule pathway (*20*). (**F**) The eukaryotic (*S. cerevisiae*) Ac/N-end rule pathway) (*9-13*). (**G**) The eukaryotic (*S. cerevisiae*) Arg/N-end rule pathway (*10*, *12*, *15*, *23*, *28*).

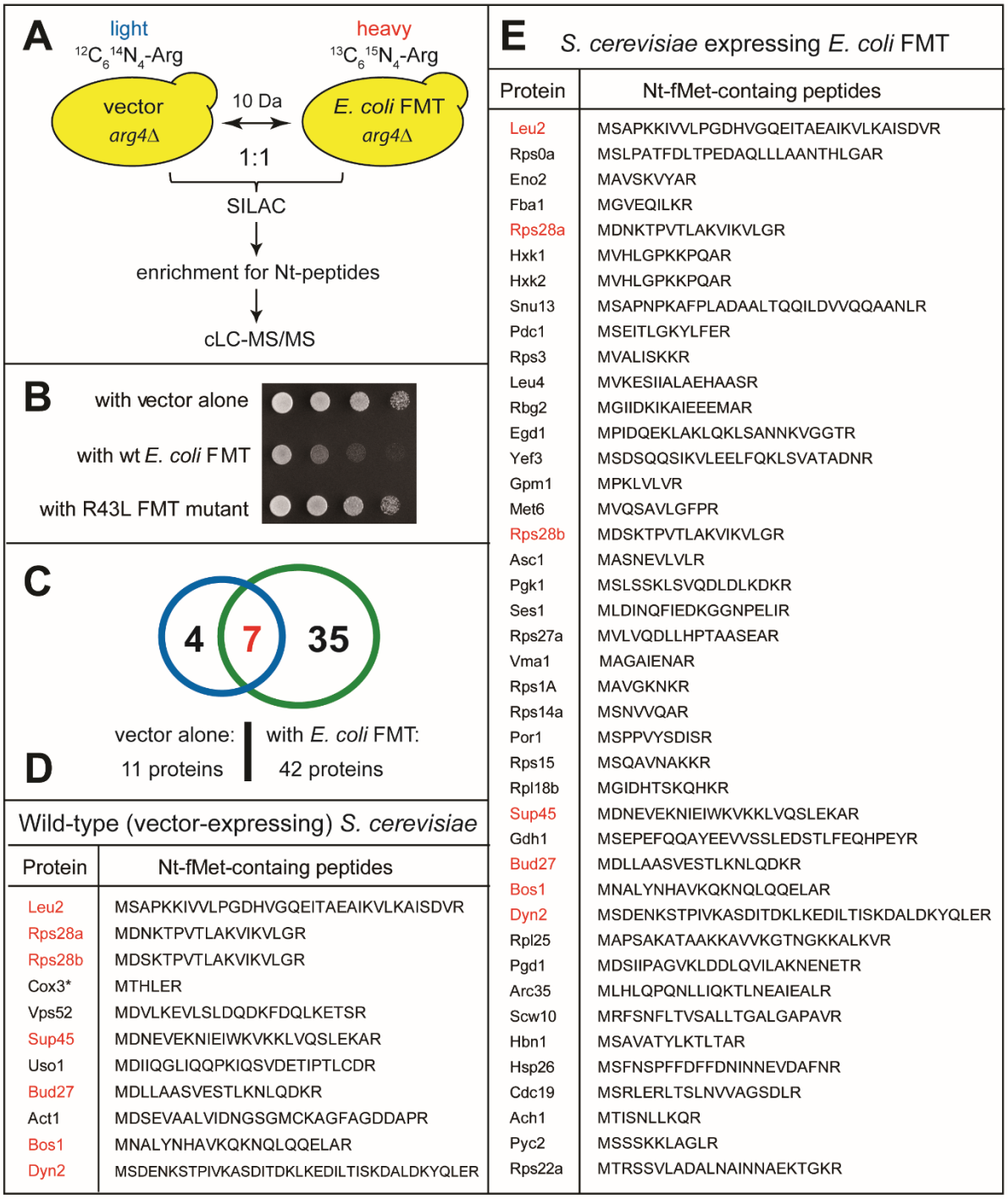

Wild-type (vector-expressing) *S. cerevisiae*

Protein	Nt-fMet-containg peptides
Leu2	MSAPKKIVVLPGDHVGQEITAEAIKVLKAISDVR
Rps28a	MDNKTPVTLAKVIKVLGR
Rps28b	MDSKTPVTLAKVIKVLGR
Cox3*	MTHLER
Vps52	MDVLKEVLSLDQDKFDQLKETSR
Sup45	MDNEVEKNIEIWKVKKLVQSLEKAR
Uso1	MDIIQGLIQQPKIQSVDETIPTLCDR
Bud27	MDLLAASVESTLKNLQDKR
Act1	MDSEVAALVIDNGSGMCKAGFAGDDAPR
Bos1	MNALYNHAVKQKNQLQQELAR
Dyn2	MSDENKSTPIVKASDITDKLKEDILTISKDALDKYQLER

E *S. cerevisiae* expressing *E. coli* FMT

Protein	Nt-fMet-containg peptides
Leu2	MSAPKKIVVLPGDHVGQEITAEAIKVLKAISDVR
Rps0a	MSLPATFDLTPEDAQLLLAANTHLGAR
Eno2	MAVSKVYAR
Fba1	MGVEQILKR
Rps28a	MDNKTPVTLAKVIKVLGR
Hxk1	MVHLGPKKPQAR
Hxk2	MVHLGPKKPQAR
Snu13	MSAPNPKAFPLADAALTQQILDVVQQAANLR
Pdc1	MSEITLGKYLFER
Rps3	MVALISKKR
Leu4	MVKESIIALAEHAASR
Rbg2	MGIIDKIKAIEEEMAR
Egd1	MPIDQEKLAKLQKLSANNKVGGTR
Yef3	MSDSQQSIKVLEELFQKLSVATADNR
Gpm1	MPKLVLVR
Met6	MVQSAVLGFPR
Rps28b	MDSKTPVTLAKVIKVLGR
Asc1	MASNEVLVLR
Pgk1	MSLSSKLSVQDLDLKDKR
Ses1	MLDINQFIEDKGGNPELIR
Rps27a	MVLVQDLLHPTAASEAR
Vma1	MAGAIENAR
Rps1A	MAVGKNKR
Rps14a	MSNVVQAR
Por1	MSPPVYSDISR
Rps15	MSQAVNAKKR
Rpl18b	MGIDHTSKQHKR
Sup45	MDNEVEKNIEIWKVKKLVQSLEKAR
Gdh1	MSEPEFQQAYEEVVSSLEDSTLFEQHPEYR
Bud27	MDLLAASVESTLKNLQDKR
Bos1	MNALYNHAVKQKNQLQQELAR
Dyn2	MSDENKSTPIVKASDITDKLKEDILTISKDALDKYQLER
Rpl25	MAPSAKATAAKKAVVKGTNGKKALKVR
Pgd1	MDSIIPAGVKLDDLQVILAKNENETR
Arc35	MLHLQPQNLLIQKTLNEAIEALR
Scw10	MRFSNFLTVSALLTGALGAPAVR
Hbn1	MSAVATYLKTLTAR
Hsp26	MSFNSPFFDFFDNINNEVDAFNR
Cdc19	MSRLERLTSLNVVAGSDLR
Ach1	MTISNLLKQR
Pyc2	MSSSKKLAGLR
Rps22a	MTRSSVLADALNAINNAEKTGKR

Fig. S2. Proteomic analyses of Nt-formylated proteins. (**A**) Diagram of a quantitative proteomic analysis that used SILAC, enrichment for N-terminal (Nt) peptides and tandem mass spectrometry. *S. cerevisiae* (*arg4Δ*) expressing *Ec*FMT were grown in a "heavy" medium ($^{13}C_6$-Arg), while the control *arg4Δ S. cerevisiae*, carrying vector alone, were grown in the

otherwise identical "light" medium ($^{12}C_6$-Arg). Equal numbers of cells from heavy and light media were mixed before preparation of cell extracts, protease digestion, enrichment for Nt-peptides and capillary liquid chromatography-tandem mass spectrometry (cLC-MS/MS) (see Materials and methods and table S1). (**B**) Growth of *S. cerevisiae* was decreased by ectopic expression of *Ec*FMT but not by expression of its catalytically inactive *Ec*FMT^{R43L} mutant. (**C**) Venn diagram indicating the numbers of specific Nt-formylated proteins identified by cLC-MS/MS analyses in the control (vector alone) vs. *Ec*FMT-expressing *S. cerevisiae*. (**D**) The identified Nt-fMet-bearing proteins in *S. cerevisiae* that expressed vector alone. (**E**) The identified Nt-fMet-bearing proteins in *Ec*FMT-expressing *S. cerevisiae*.

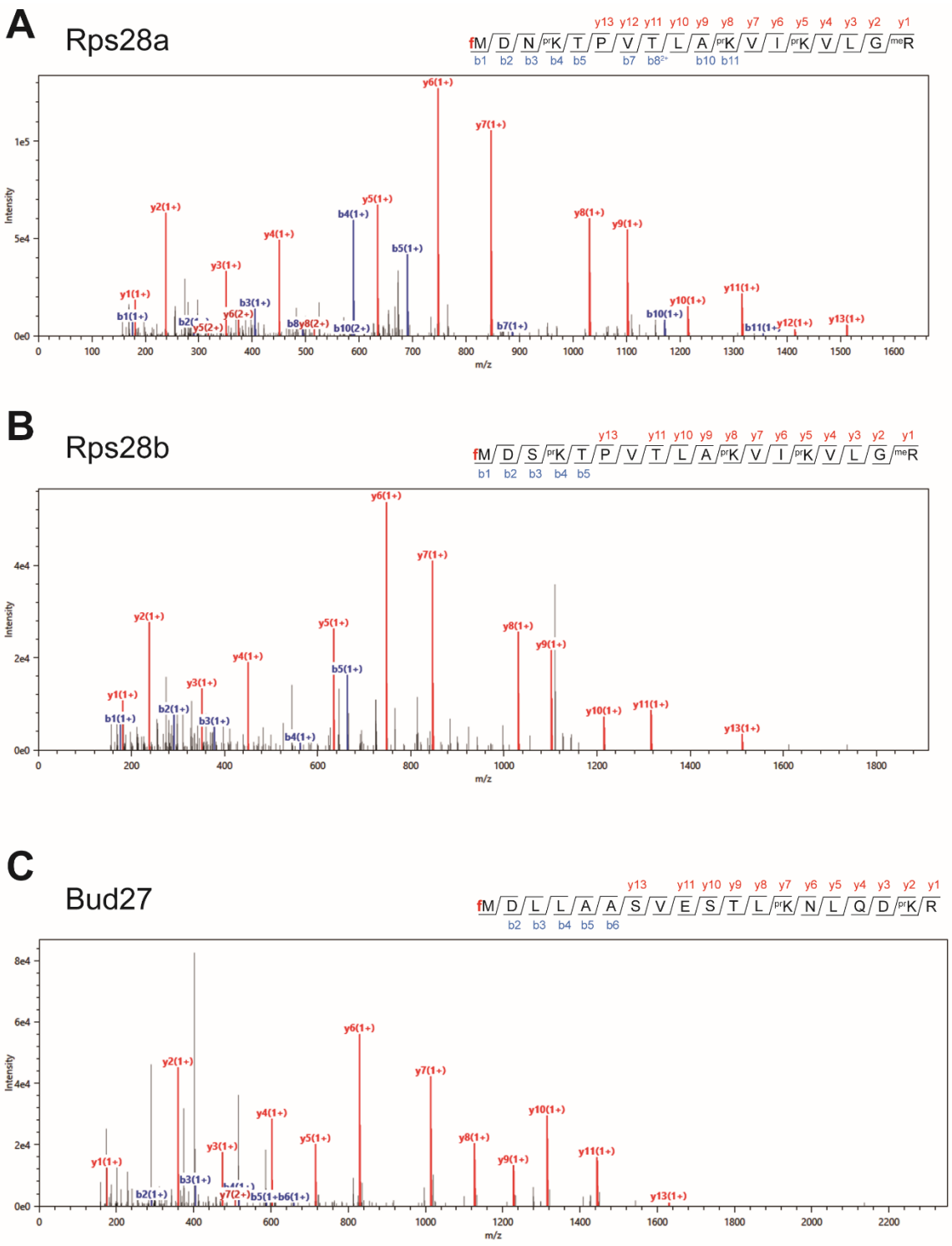

Fig. S3 (A-C, multi-page S-figure). **Mass spectrometric analyses of Nt-formylated proteins from wild-type (lacking *Ec*FMT) *S. cerevisiae*.** (**A**) Rps28a, a ribosomal protein. (**B**) Rps28b, a ribosomal protein. (**C**) Bud27, a bud site selection protein. See Materials and methods.

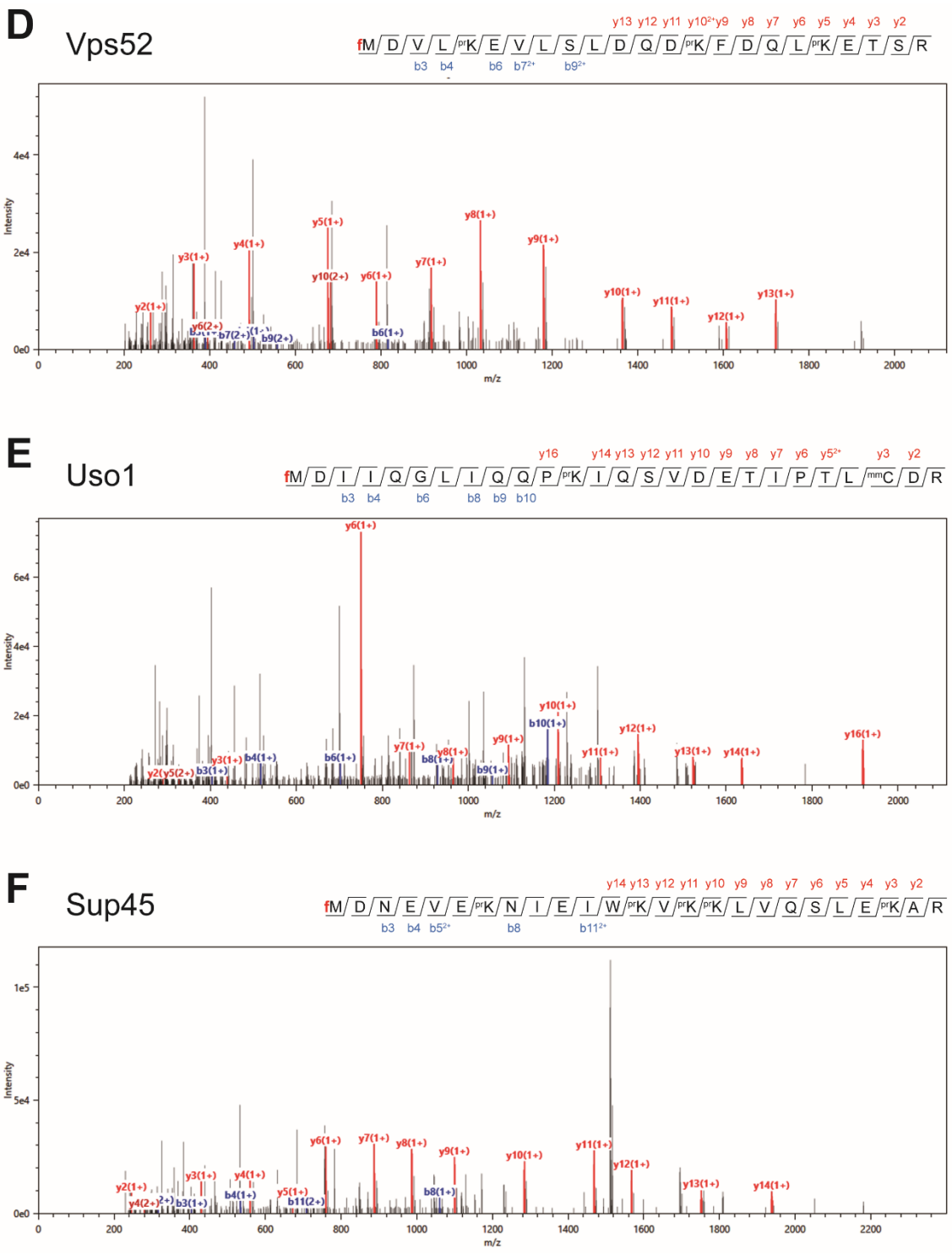

Fig. S3 (D-F, multi-page S-figure). **Mass spectrometric analyses of Nt-formylated proteins from wild-type (lacking *Ec*FMT) *S. cerevisiae*.** (**D**) Vps52, a vacuolar-sorting associated protein. (**E**) Uso1, a vesicle transporter. (**F**) Sup45, a peptide chain release factor subunit. See Materials and methods.

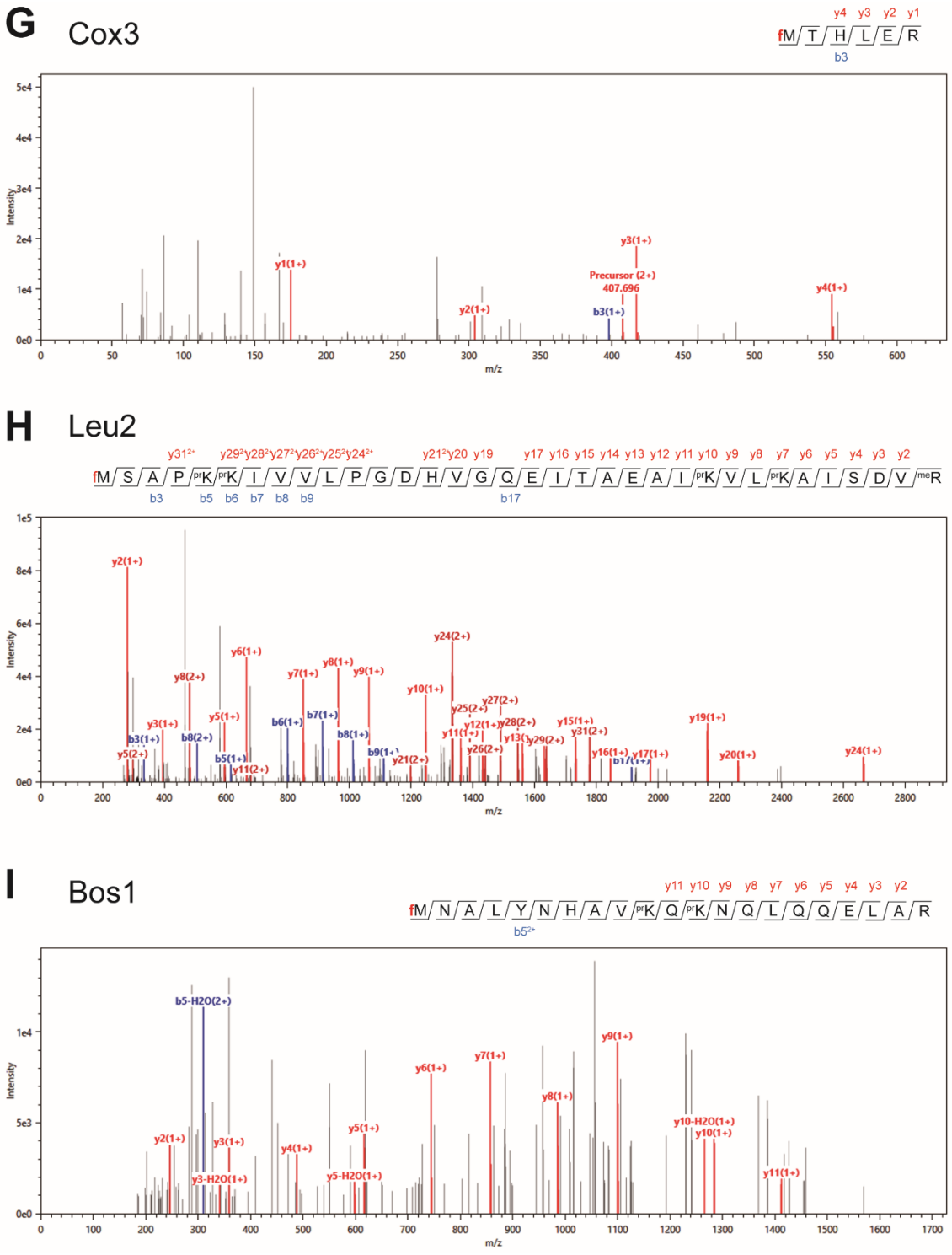

Fig. S3 (G-I, multi-page S-figure). **Mass spectrometric analyses of Nt-formylated proteins from wild-type (lacking *Ec*FMT) *S. cerevisiae*.** (**G**) Cox3, a cytochrome c oxidase subunit, the mitochondrial DNA-encoded protein. (**H**) Leu2, 3-isopropyl malate dehydrogenase. (**I**) Bos1, a vesicle-specific SNAP receptor. See Materials and methods.

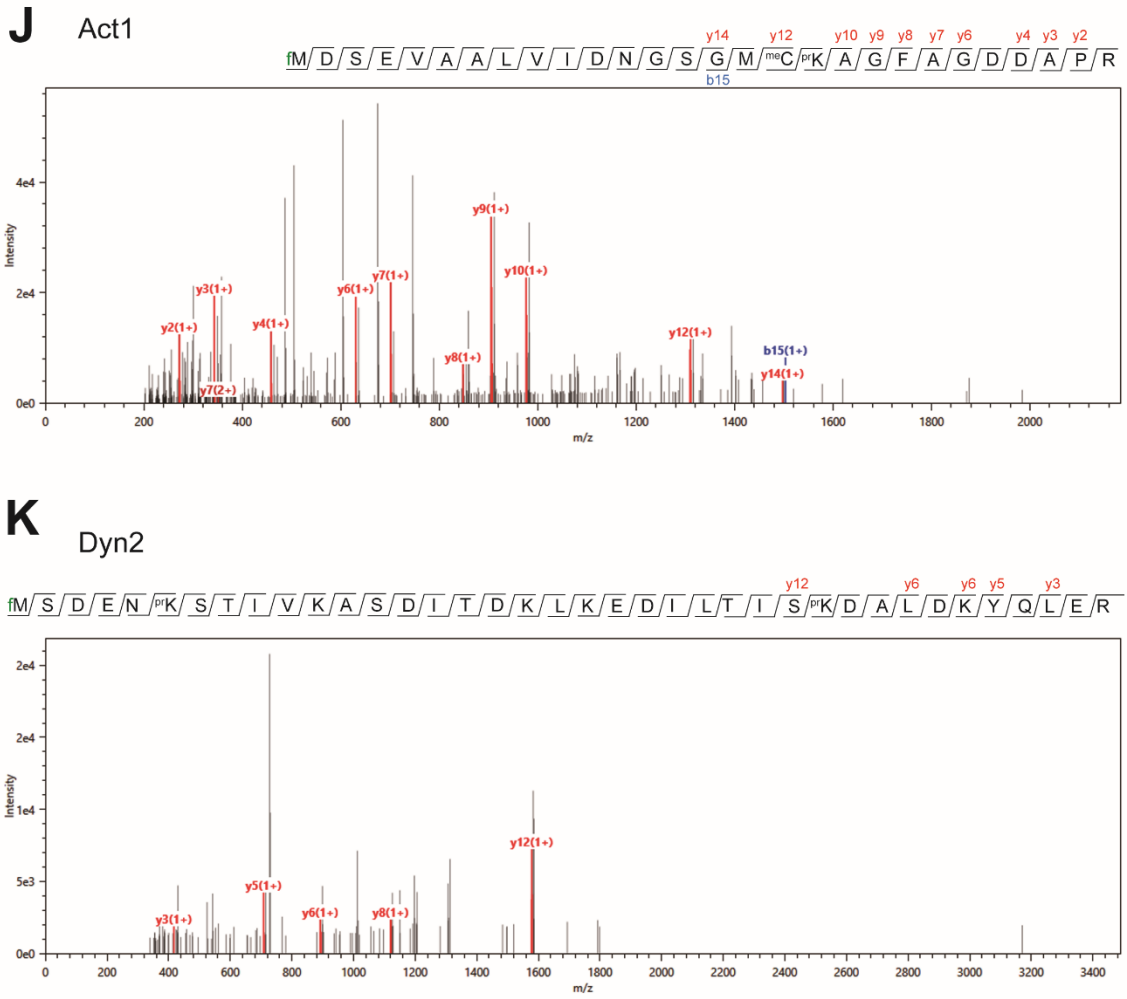

Fig. S3 (J-K, multi-page S-figure). **Mass spectrometric analyses of Nt-formylated proteins from wild-type (lacking *Ec*FMT) *S. cerevisiae*.** (**J**) Act1, actin. (**K**) Dyn2, a dynein light chain. See Materials and methods.

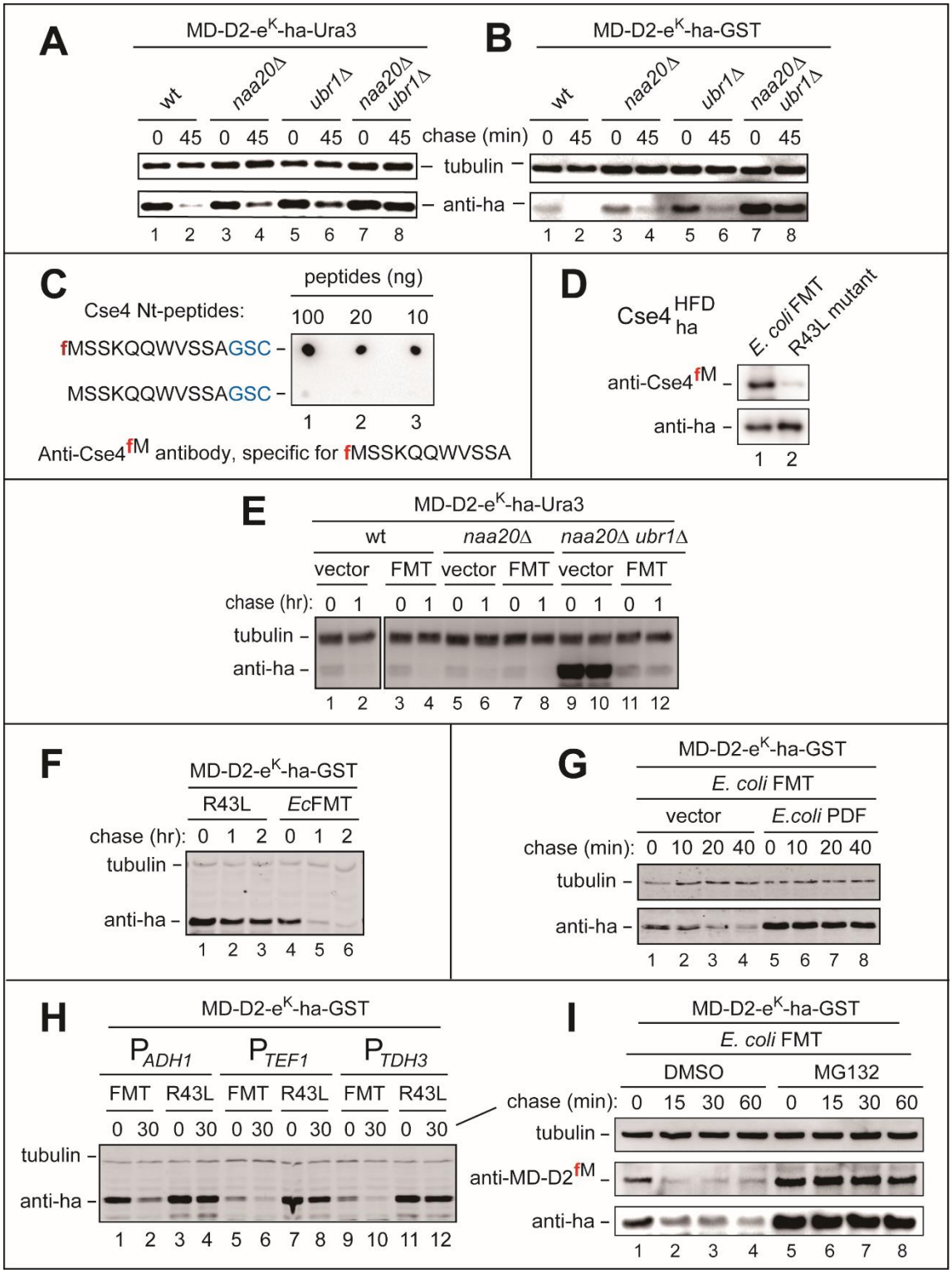

Fig. S4. Analyses of Nt-formylation reporters in wild-type, *naa20Δ ubr1Δ*, and *Ec*FMT-expressing *S. cerevisiae.* (**A**) See Fig. 1A for the diagram of reporter proteins. CHX-chases of MD-D2-e^K-ha-Ura3 in wild-type, *naa20Δ*, *ubr1Δ*, and double-mutant *naa20Δ ubr1Δ*

S. cerevisiae in SC medium. Note the instability of MD-D2-e^K-ha-Ura3 in wild-type yeast and its nearly complete stabilization in *naa20Δ ubr1Δ* cells, which grew at nearly wild-type rates. See also the main text. In these and other immunoblotting experiments, immunoblots with anti-tubulin antibody served as loading controls. (**B**) Same as in **A** but with MD-D2-e^K-ha-GST. (**C**) Dot immunoblotting with affinity-purified anti-Cse4^{fM} antibody, the synthetic Nt-formylated peptide fMSSKQQWVSSAGSC and its unformylated counterpart MSSKQQWVSSAGSC. The sequence of these peptides, save for the three (underlined) C-terminal residues, was identical to the sequence of the 11 Nt-residues of *S. cerevisiae* Cse4. Note specific binding of anti-Cse4^{fM} to Nt-formylated fMSSKQQWVSSAGSC. See also the main text, and Materials and methods. (**D**) Immunoblotting, using anti-Cse4^{fM} and anti-ha antibodies, of SDS-PAGE-fractionated extracts from *psh1Δ S. cerevisiae* that expressed the "hybrid" $Cse4^{HFD}_{ha}$ histone (see the main text and Fig. 3C), as well as either wild-type *Ec*FMT or its catalytically inactive *Ec*FMT^{R43L} mutant. (**E**) CHX-chases, using anti-ha, with MD-D2-e^K-ha-Ura3 in wild-type, *naa20Δ*, and *naa20Δ ubr1Δ S. cerevisiae* that expressed either vector alone or wild-type *Ec*FMT from the P_{GAL1} promoter on a high copy plasmid in SGal medium. (**F**) CHX-chases, using anti-ha, with MD-D2-e^K-ha-GST in *naa20Δ ubr1Δ S. cerevisiae* that expressed either wild-type *Ec*FMT (lanes 4-6) or its catalytically inactive *Ec*FMT^{R43L} mutant (lanes 1-3). (**G**) CHX-chases, using anti-ha, with MD-D2-e^K-ha-GST in *naa20Δ ubr1Δ S. cerevisiae* that expressed wild-type *Ec*FMT in either the absence (lanes 1-4) or presence (lanes 5-8) of the wild-type *Ec*PDF deformylase. (**H**) CHX-chases with MD-D2-e^K-ha-GST in *naa20Δ ubr1Δ S. cerevisiae* that expressed either wild-type *Ec*FMT or its inactive *Ec*FMT^{R43L} mutant from the incrementally stronger yeast promoters P_{ADH1}, P_{TEF1}, and P_{TDH3}. (**I**) CHX-chases, using anti-MD-D2^{fM}, anti-ha, and anti-tubulin antibodies, with MD-D2-e^K-ha-GST in *Ec*FMT expressing *naa20Δ ubr1Δ S. cerevisiae* in the presence of either DMSO (control; lanes 1-4) or the MG132 proteasome inhibitor dissolved in DMSO (lanes 5-8).

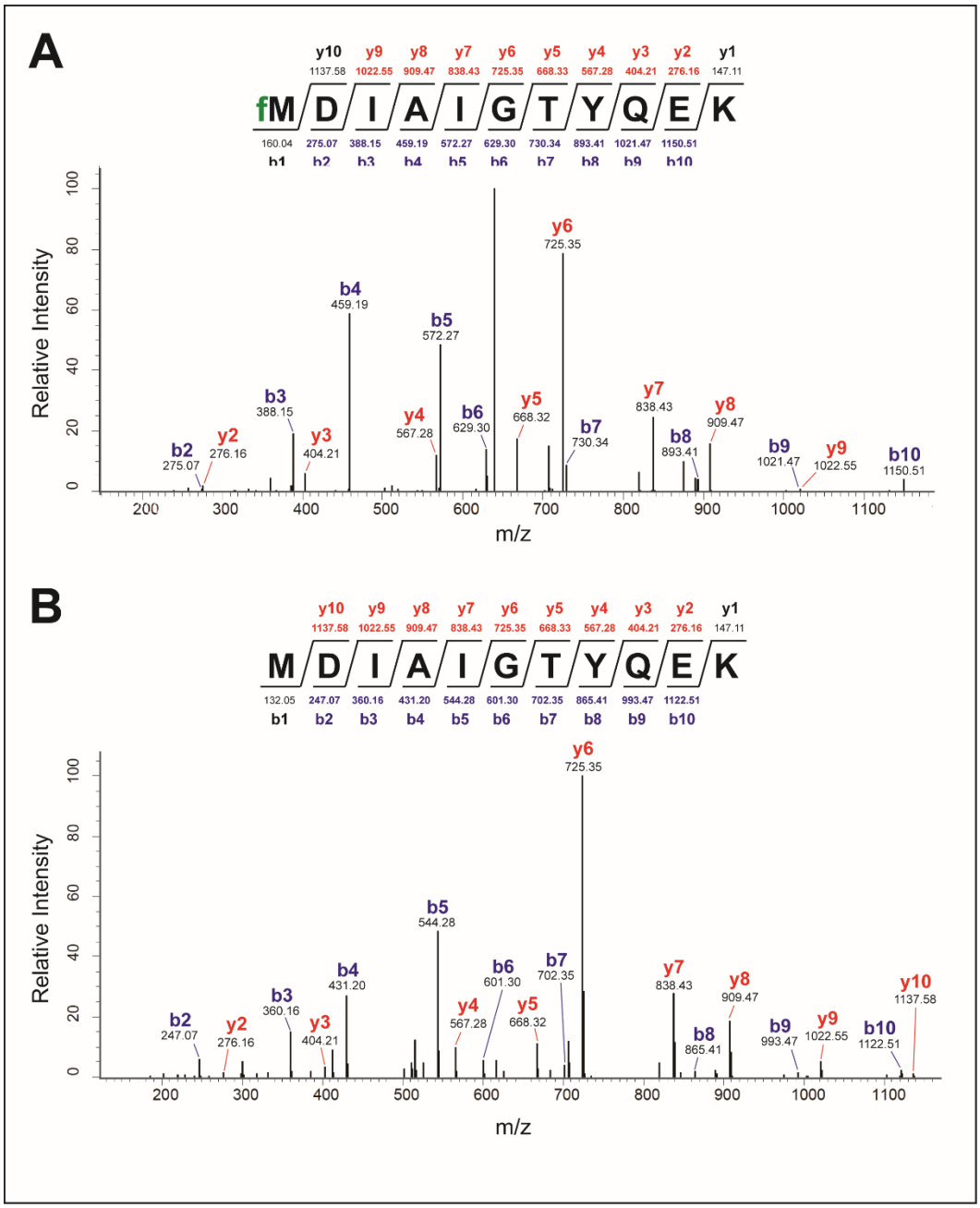

Fig. S5. Mass spectrometric analyses of Nt-formylated fMD-D2-GST. (**A**) Nt-formylated fMD-D2-GST was expressed in *E. coli* in the presence of actinonin, an inhibitor of the PDF, was purified as described in Materials and methods, and was analyzed for its Nt-formylation state using cLC-MS/MS. (**B**) Same as in **A**, but no actinonin during expression and isolation of MD-D2-GST.

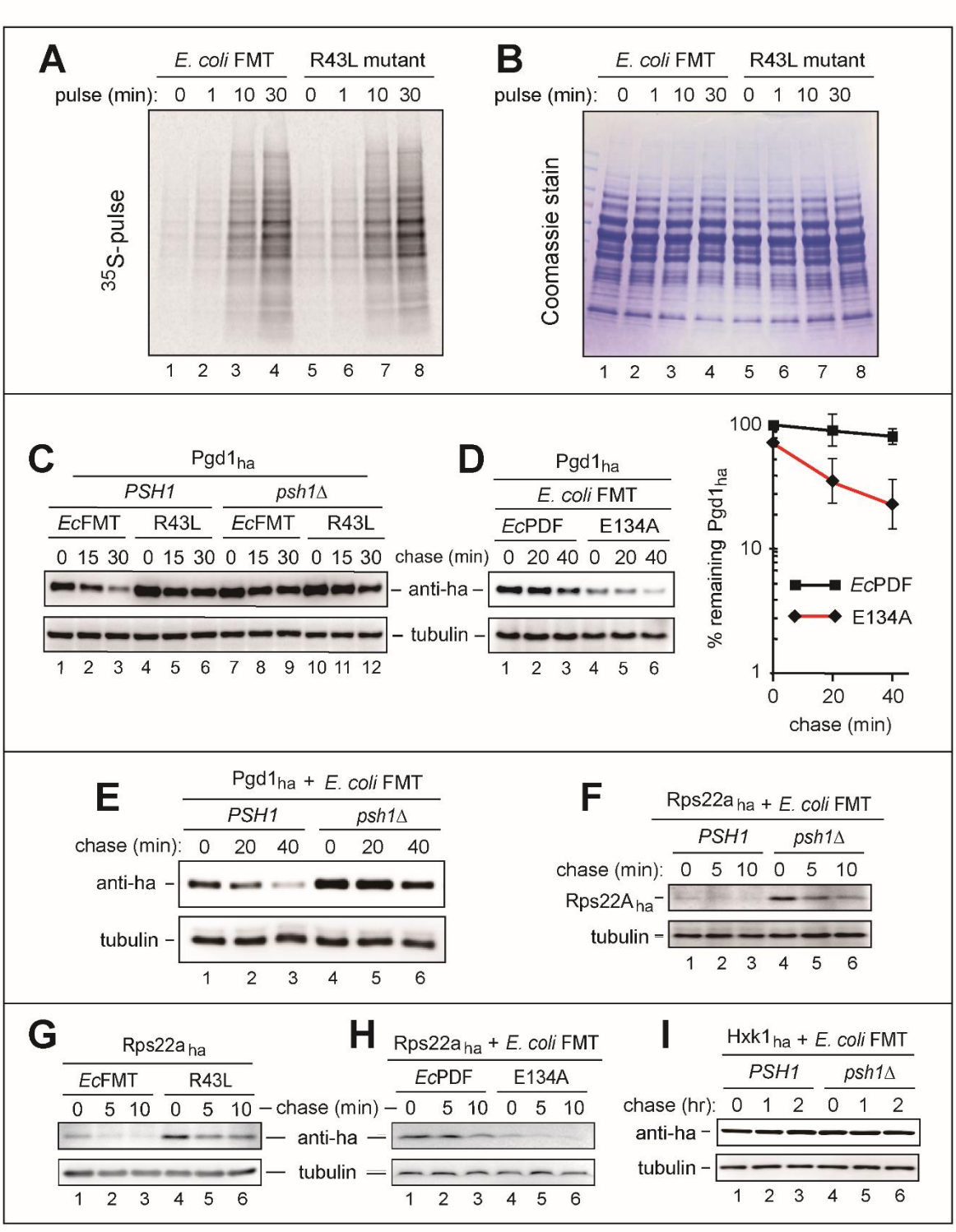

Fig. S6. Ectopic expression of *Ec*FMT has no significant effect on the rate of protein synthesis in *S. cerevisiae*. (**A**) *naa20Δ ubr1Δ* cells that expressed either *Ec*FMT (lanes 1-4) or its catalytically inactive *Ec*FMT^{R43L} mutant (lanes 5-8) from a low copy plasmid and the P_{ADH1} promoter were labelled with ^{35}S-Met/Cys for indicated times. Extracts from identical amounts of

cells after pulses of ^{35}S-Met/Cys were subjected to SDS-PAGE, and fractionated proteins were detected by autoradiography. (**B**) Same as in **A**, but the gel was stained with Coomassie. (**C**) CHX-chases, using anti-ha, with $Pgd1_{ha}$ in wild-type and *psh1Δ S. cerevisiae* that expressed either wild-type *Ec*FMT or its catalytically inactive *Ec*FMT^{R43L} mutant, as indicated. (**D**) CHX-chases, using anti-ha, with $Pgd1_{ha}$ in wild-type *S. cerevisiae* that expressed wild-type *Ec*FMT together with either wild-type *Ec*PDF or its catalytically inactive *Ec*PDF^{E134A} mutant. The graphs show quantification of data (three independent pairs of CHX-chases), with mean ± standard error (SE). (**E**) CHX-chases, using anti-ha, with $Pgd1_{ha}$ in wild-type (*PSH1*) (lanes 1-3) and *psh1Δ* (lanes 4-6) *Ec*FMT-expressing *S. cerevisiae*. (**F**) CHX-chases, using anti-ha, with $Rps22a_{ha}$ in wild-type (*PSH1*) (lanes 1-3) and *psh1Δ* (lanes 4-6) *Ec*FMT-expressing *S. cerevisiae*. (**G**) CHX-chases, using anti-ha, with $Rps22a_{ha}$ in wild-type *S. cerevisiae* that expressed either the wild-type *Ec*FMT (lanes 1-3) or its inactive *Ec*FMT^{R43L} mutant (lanes 4-6). (**H**) CHX-chases using anti-ha, with $Rps22a_{ha}$ in wild-type (*PSH1*) *S. cerevisiae* that expressed the wild-type *Ec*FMT together with either the wild-type *Ec*PDF (lanes 1-3) or its catalytically inactive *Ec*PDF^{E134A} mutant (lanes 4-6). (**I**) CHX-chases, using anti-ha, with $Hxk1_{ha}$ in *Ec*FMT-expressing wild-type (*PSH1*) (lanes 1-3) and *psh1Δ* (lanes 4-6) *S. cerevisiae*.

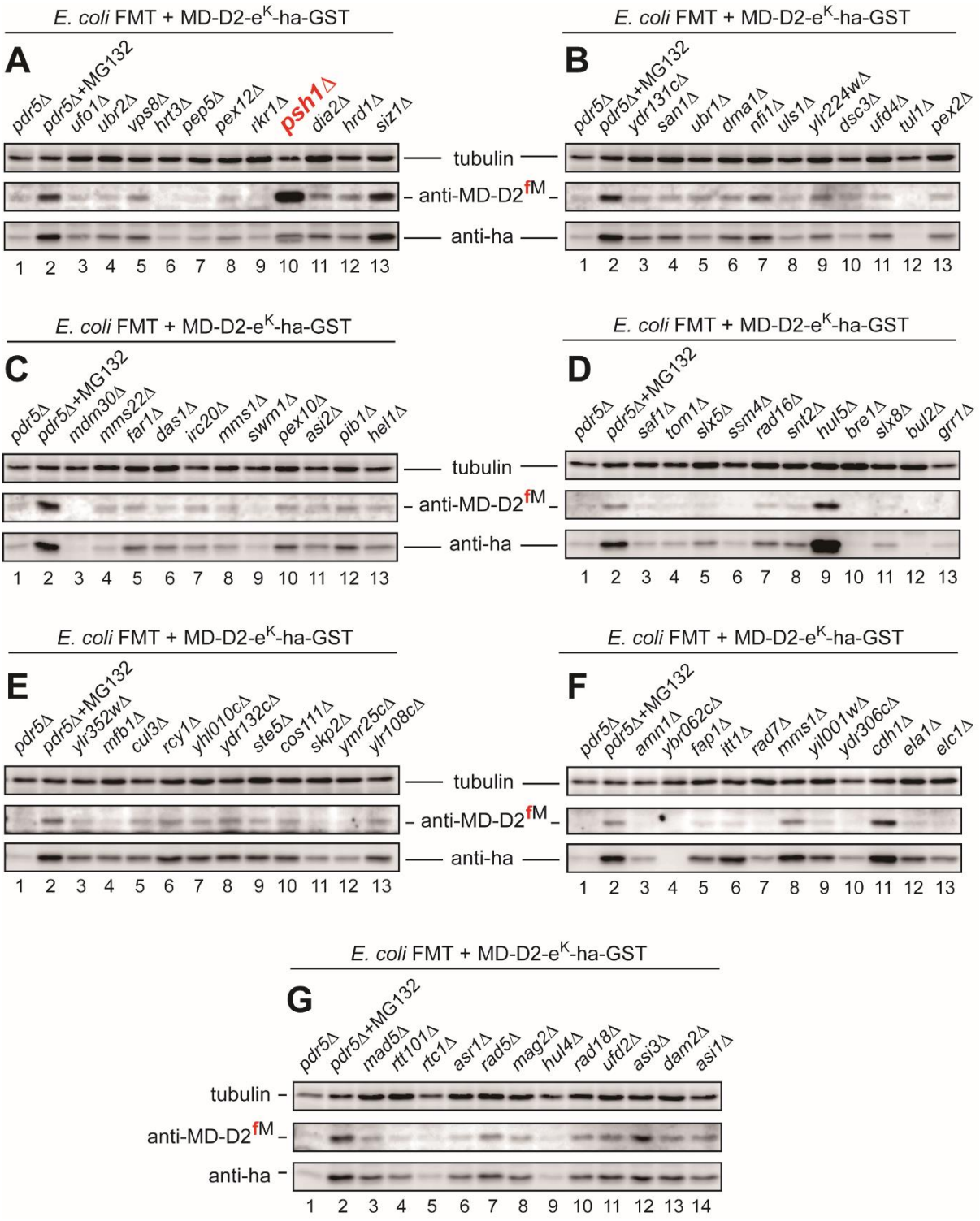

Fig. S7. Screening for a ubiquitin ligase that mediates the *S. cerevisiae* fMet/N-end rule pathway. (**A-G**) A collection of single-mutant BY4741-based *S. cerevisiae* strains was used that lacked specific E3 Ub ligases and expressed both the Nt-formylation reporter MD-D2-e^{K}-ha-GST and *Ec*FMT. The latter was used to augment the synthesis of Nt-formylated

proteins. Extracts from the indicated 78 mutant strains were fractionated by SDS-PAGE and immunoblotted with anti-ha, anti-MD-D2^{fM}, and anti-tubulin. Anti-ha detected all species of MD-D2-e^{K}-ha-GST, whereas anti-MD-D2^{fM} selectively detected fMD-D2-e^{K}-ha-GST. Marked in red, in lane A10, is the result that identified Psh1 as the E3 Ub ligase of the fMet/N-end rule pathway. See also the main text.

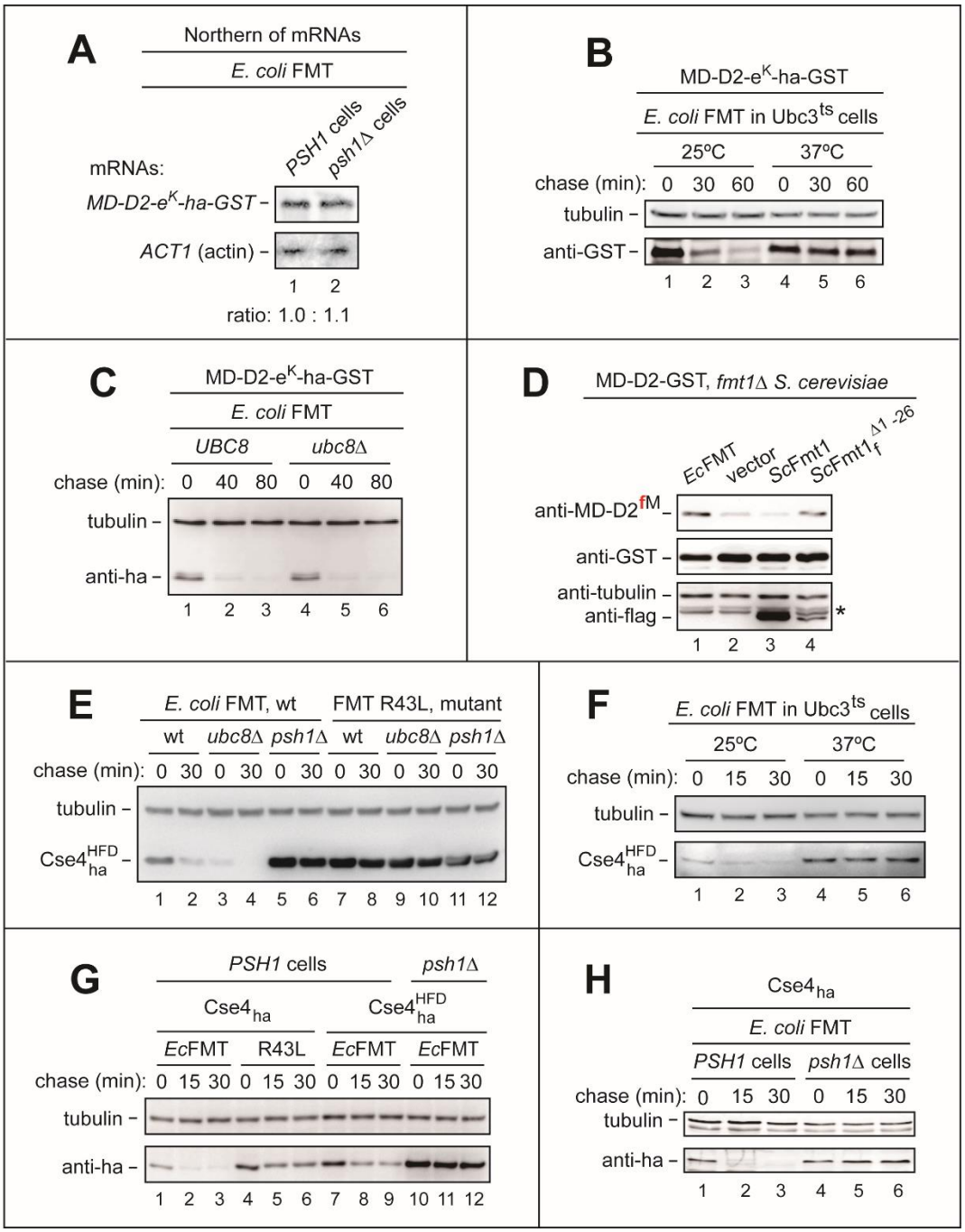

Fig. S8. The Psh1 E3 ubiquitin ligase and Cse4, its physiological substrate.
(**A**) Approximately equal levels of mRNA encoding MD-D2-e^{K}-ha-GST in *PSH1* and *psh1Δ S. cerevisiae*, as determined by Northern hybridization (see Materials and methods). (**B**) CHX-chases, using anti-GST, at 25°C (lanes 1-3) and at 37°C (lanes 4-6), with MD-D2-e^{K}-ha-GST in *Ec*FMT-expressing *PSH1 S. cerevisiae* that was a temperature-sensitive Ubc3^{ts} mutant (see the main text). (**C**) CHX-chases, using anti-ha, with MD-D2-e^{K}-ha-GST in *Ec*FMT-expressing *PSH1 S. cerevisiae* that either contained (lanes 1-3) or lacked (lanes 4-6) the

Ubc8 E2 enzyme (see the main text). (**D**) The relative levels of Nt-formylated MD-D2-GST (upper panel), determined using anti-MD-D2^{fM}, in *fmt1Δ S. cerevisiae* that was grown to A_{600} of ~1 and expressed either wild-type *Ec*FMT (lane 1), or vector alone (lane 2), or C-terminally flag-tagged wild-type *Sc*Fmt1$_f$ (lane 3), or the mitochondrial presequence-lacking $Sc\mathrm{Fmt1}_{\mathrm{f}}^{\Delta 1-26}$ (lane 4). Middle and lower panels, immunoblotting with anti-GST, anti-tubulin and anti-flag, respectively. The asterisk in the lowest panel denotes a crossreacting band above the band of *Sc*Fmt1$_f$. See also the main text. (**E**) CHX-chases, using anti-ha, with $\mathrm{Cse4}_{\mathrm{ha}}^{\mathrm{HFD}}$, in *S. cerevisiae* that expressed wild-type *Ec*FMT (lanes 1-6) and either contained both Psh1 and Ubc8 (lanes 1-2), or lacked Ubc8 (lanes 3-4), or lacked Psh1 (lanes 5-6). Lanes 7-12, same as lanes 1-6 but with the same *S. cerevisiae* strains that expressed the catalytically inactive *Ec*FMT^{R43L} mutant. See also the main text. (**F**) CHX-chases, using anti-ha, at 25℃ (lanes 1-3) and at 37℃ (lanes 4-6), with $\mathrm{Cse4}_{\mathrm{ha}}^{\mathrm{HFD}}$, in *Ec*FMT-expressing *PSH1 S. cerevisiae* that was a temperature-sensitive Ubc3^{ts} mutant (see the main text). (**G**) CHX chases, using anti-ha, with Cse4$_{ha}$, in *PSH1 S. cerevisiae* that expressed either wild-type *Ec*FMT (lanes 1-3) or its inactive *Ec*FMT^{R43L} mutant (lanes 4-6). Lanes 7-9, same as lanes 1-3 but with $\mathrm{Cse4}_{\mathrm{ha}}^{\mathrm{HFD}}$. Lanes 10-12, same as lanes 7-9, but with *psh1Δ S. cerevisiae.* (**H**) CHX chases, using anti-ha, with Cse4$_{ha}$, in *PSH1* (lanes 1-3) or *psh1Δ* (lanes 4-6) *S. cerevisiae* that expressed wild-type *Ec*FMT.

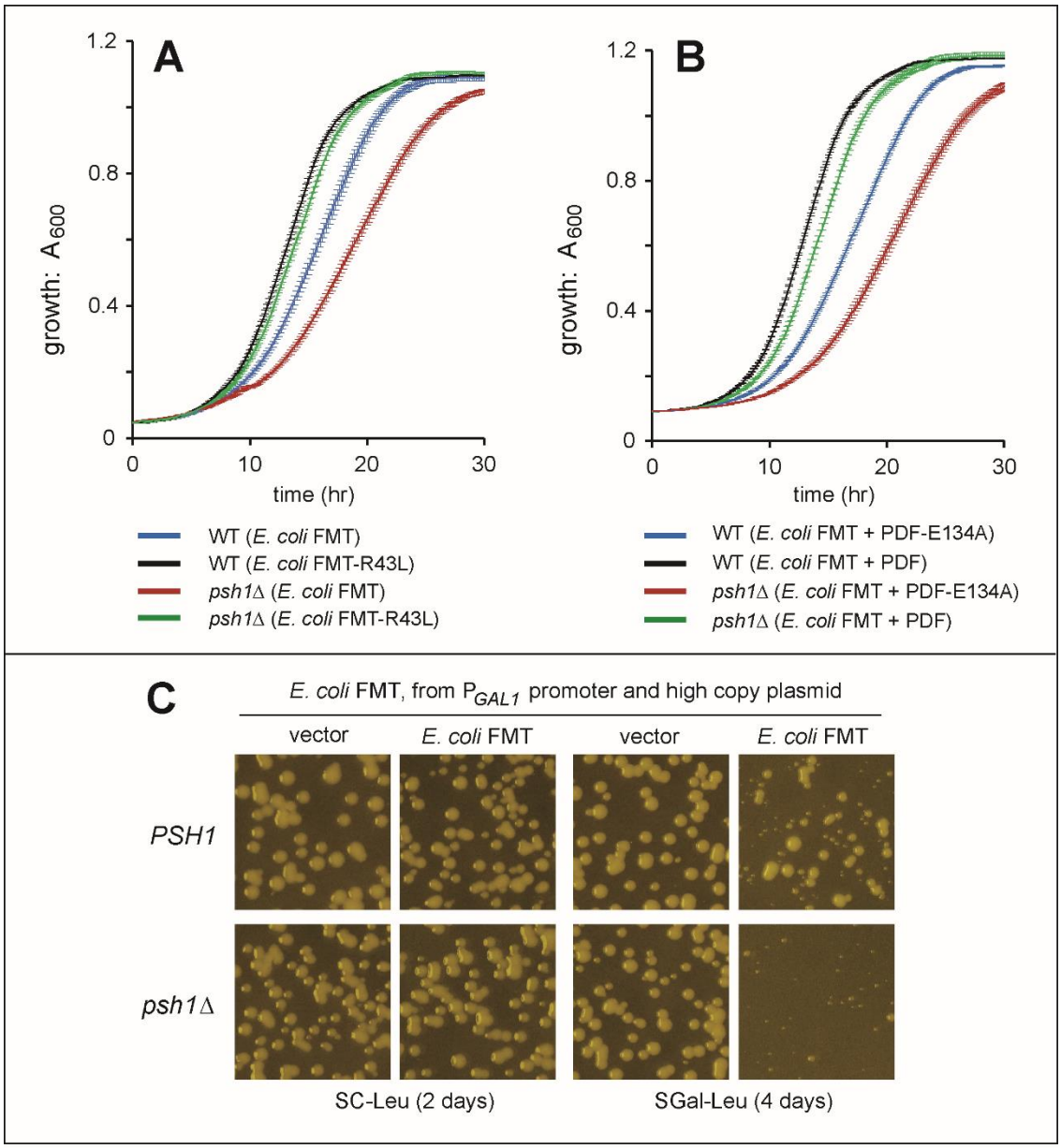

Fig. S9. Psh1-mediated destruction of Nt-formylated proteins counteracts their toxicity. (**A**) Growth rates of wild-type (*PSH1*) and *psh1Δ S. cerevisiae* that expressed either wild-type *Ec*FMT or its inactive *Ec*FMT^{R43L} mutant in SC medium. (**B**) Same as in **A**, but wild-type (*PSH1*) and *psh1Δ S. cerevisiae* that expressed wild-type *Ec*FMT together with either wild-type *Ec*PDF or its inactive *Ec*PDF^{E134A} mutant. In both **A** and **B**, each point of a curve also indicates ± standard error (SE) of A_{600} measurements (at 10-min intervals) that were carried out independently six times (see Materials and methods). (**C**) Colony growth assay. Approximately 500 cells of wild-type (*PSH1*) and *psh1Δ S. cerevisiae* carrying either vector alone (p425GAL) or pCH3082 (expressing wild-type *Ec*FMT) were spread onto SC(-Leu) plates (no expression of *Ec*FMT) or onto SGal(-Leu) plates (expression of *Ec*FMT), followed by incubation at 30℃ for 2 and 4 days, respectively.

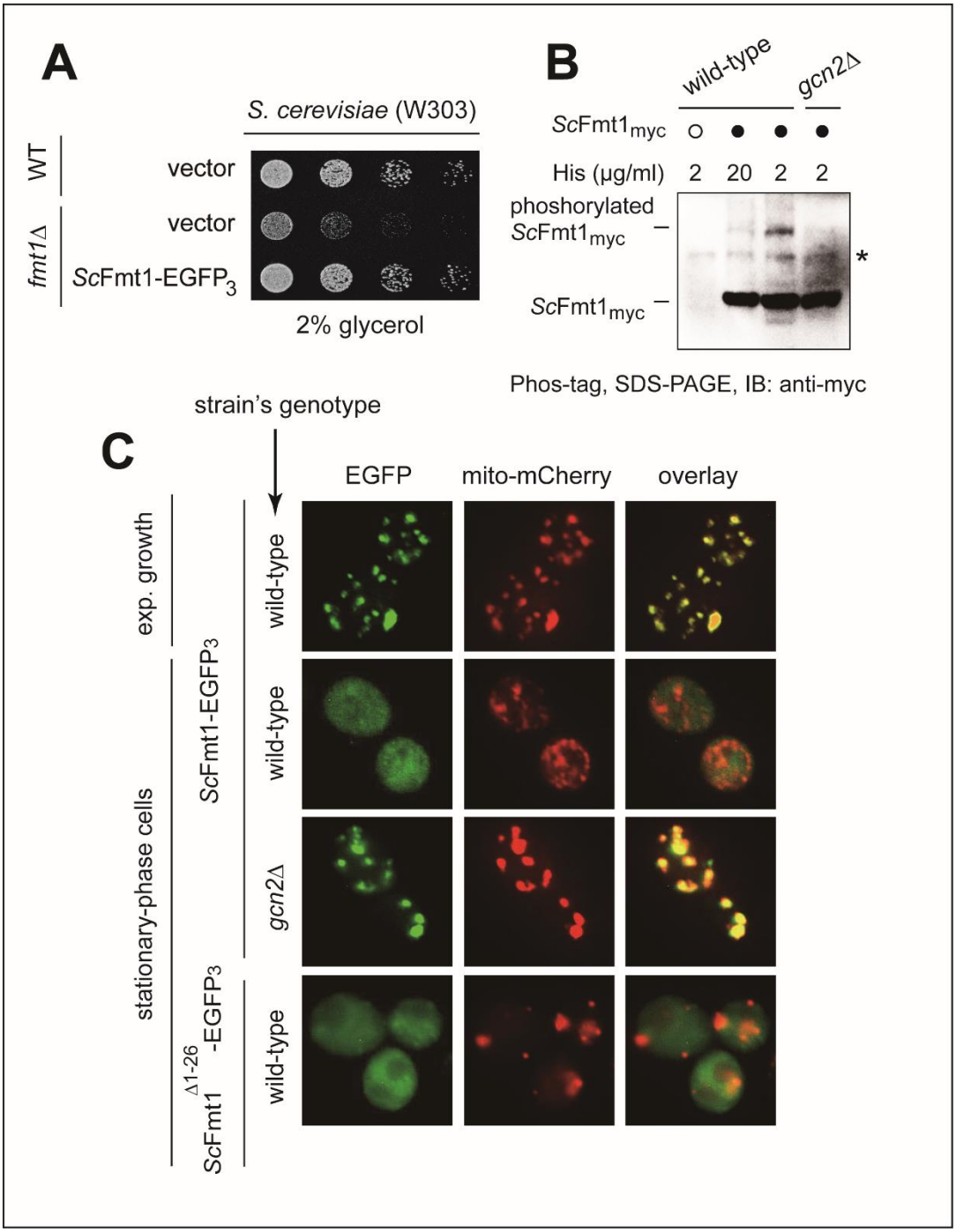

Fig. S10. Localization of *Sc*Fmt1 in growing and stationary-phase wild-type and *gcn2Δ* cells. (**A**) *Sc*Fmt1-EGFP$_3$ functionally complemented the impaired growth of *fmt1Δ* W303 *S. cerevisiae* on respiratory minimal medium containing nonfermentable 2% glycerol. (**B**) A Phos-tag analysis for the validation of *Sc*Fmt1 phosphorylation. Wild-type and *gcn2Δ* cells that expressed either vector alone or *Sc*Fmt1$_{myc}$ (as indicated) were grown for 24 hr at 30°C in SC medium supplemented with either 20 μg/ml or 2 μg/ml of histidine (His), as indicated. Extracts of wild-type and *gcn2Δ* cells were subjected to Phos-tag SDS-PAGE followed by

immunoblotting with anti-myc antibody (see Materials and methods). An asterisk denotes a non-specific band. (**C**) Representative images of fluorescent wild-type or *gcn2Δ S. cerevisiae* cells that coexpressed mito-mCherry (a mitochondrial marker) and either the presequence-lacking *Sc*Fmt1$^{\Delta 1\text{-}26}$-EGFP$_3$ fusion or "wild-type" *Sc*Fmt1-EGFP$_3$ either in exponential growth or in stationary phase, as indicated. Note the increased cytosolic localization of "wild-type" *Sc*Fmt1-EGFP$_3$ in wild-type stationary-phase cells but not in stationary-phase *gcn2Δ* cells.

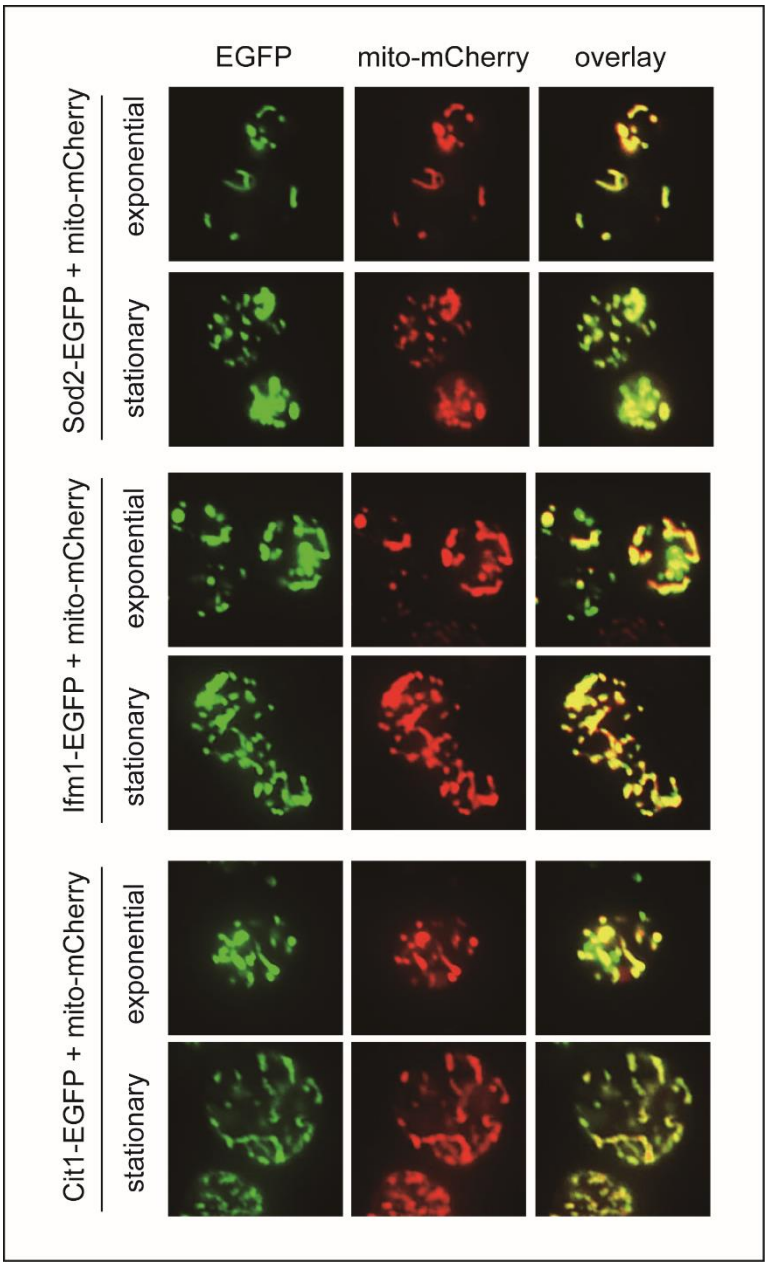

Fig. S11. Localization of nuclear DNA-encoded but mitochondrial matrix-targeting proteins in the stationary phase. Representative images of fluorescent wild-type *S. cerevisiae* cells that coexpressed mito-mCherry (a mitochondrial marker) and C-terminal fusions of EGFP to the yeast mitochondrial-matrix proteins Sod2, Ifm1, and Cit1. Note that the bulk of these nuclear DNA-encoded mitochondrial-matrix proteins (their EGFP fusions) continued to reside in mitochondria in stationary-phase wild-type cells, in contrast to a strongly increased cytosolic localization of the also nuclear-DNA-encoded *Sc*Fmt1-EGFP$_3$. See also Fig. 4, C and D, and fig. S10C).

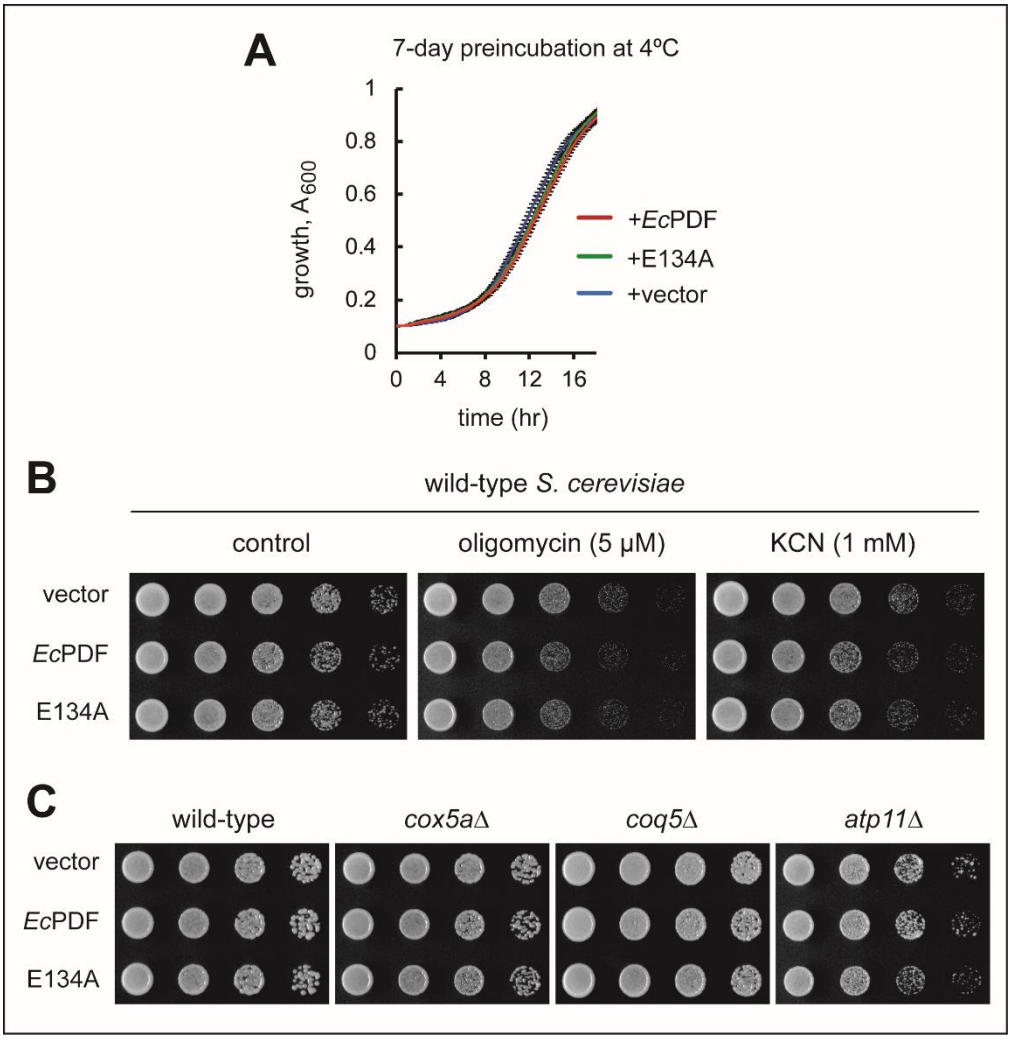

Fig. S12. Deformylation by *Ec*PDF did not affect the growth of *S. cerevisiae* strains with defects in mitochondrial function. (**A**) Growth (A_{600}) of wild-type yeast in SC medium (see Materials and methods) that expressed either the vector alone, or *Ec*PDF, or its inactive *Ec*PDF^{E134A} mutant after pre-incubation of yeast (kept as streaked-out cultures on plates) for 7 days at 4°C (in contrast to pre-incubation for 14 days at 4°C; see Fig. 5D). (**B**) Ectopic expression of either a vector alone, or *Ec*PDF, or its inactive *Ec*PDF^{E134A} mutant did not affect the growth of wild-type S. *cerevisiae* on galactose-containing minimal medium (SGal) plates (after pre-incubation of yeast, kept as streaked-out cultures on plates for 14 days at 4°C before these growth assays) with the indicated mitochondrial respiration inhibitors oligomycin or KCN. Note the difference between these results and otherwise identical tests with Na-azide (see Fig. 5E). (**C**) No inhibitors. Either wild-type *S. cerevisiae* or its *cox5aΔ* (cytochrome c oxidase subunit 5-lacking), or *coq5Δ* (coenzyme Q5-lacking), or *atp11Δ* (an F1-ATPase assembly chaperon-lacking) mutants that expressed either the vector alone, or *Ec*PDF, or its inactive *Ec*PDF^{E134A} mutant. Yeast were grown in liquid SC for 24 hr at 30°C, followed by spotting assays on SGal. The plates incubated for 2 days at 30°C.

Table S1. fMet-containing N-terminal peptides, identified using SILAC/N-terminome analysis with wild-type *S. cerevisiae* that expressed either vector alone (L, Light) or *E. coli* formyltransferase (*Ec*FMT) (H, Heavy) (see the main text and Materials and methods).

Proteins	Identified fMet-containing peptides	vector (L)[a]	*Ec*FMT (H)[a]	vector (L)[b]	*Ec*FMT (H)[b]	ratio[c] (H)[a+b]/(L)[a+b]	ratio[c] fMet (L)[a+b] /non-fMet	ratio[c] fMet (H)[a+b] /non-fMet
Cox3	MTHLER	2	0	3	0	0	n/a*	0
Cdc19	MSRLERLTSLNVVAGSDLR	0	1	0	0	n/a*	0	0.167
Pgk1	MSLSSKLSVQDLDLKDKR	0	6	0	2	n/a	0	n/a*
Eno2	MAVSKVYAR	0	37	0	31	n/a	0	n/a
Gpm1	MPKLVLVR	0	10	0	0	n/a	0	n/a
Leu2	MSAPKKIVVLPGDHVGQEITAEAIKV LKAISDVR	14	58	15	70	4.4	1.825	128
Rpl25	MAPSAKATAAKKAVVKGTNGKKAL KVR	0	1	0	0	n/a	0	n/a
Hxk1	MVHLGPKKPQAR	0	22	0	14	n/a	0	n/a
Por1	MSPPVYSDISR	0	3	0	1	n/a	0	4
Met6	MVQSAVLGFPR	0	5	0	4	n/a	0	n/a
Rps3	MVALISKKR	0	15	0	4	n/a	0	n/a
Pdc1	MSEITLGKYLFER	0	14	0	8	n/a	0	n/a
Leu4	MVKESIIALAEHAASR	0	14	0	5	n/a	0	n/a
Rps14a	MSNVVQAR	0	2	0	2	n/a	0	n/a
Gdh1	MSEPEFQQAYEEVVSSLEDSTLFEQH PEYR	0	1	0	1	n/a	0	0.667
Ses1	MLDINQFIEDKGGNPELIR	0	6	0	1	n/a	0	0.408
Rps22a	MTRSSVLADALNAINNAEKTGKR	0	1	0	0	n/a	0	n/a
Rps28b	MDSKTPVTLAKVIKVLGR	9	4	1	4	0.8	0.058	0.055
Rpl18b	MGIDHTSKQHKR	0	2	0	1	n/a	0	n/a
Sup45	MDNEVEKNIEIWKVKKLVQSLEKAR	2	2	0	0	1	0.08	0.083
Fba1	MGVEQILKR	0	35	0	16	n/a	0	n/a
Hsp26	MSFNSPFFDFFDNINNEVDAFNR	0	0	0	1	n/a	0	1

Yef3	MSDSQQSIKVLEELFQKLSVATADNR	0	7	0	5	n/a	0	6
Vma1	MAGAIENAR	0	2	0	2	n/a	0	0
Bos1	MNALYNHAVKQKNQLQQELAR	1	1	0	0	1	0.63	0.63
Uso1	MDIIQGLIQQPKIQSVDETIPTLCDR	1	0	0	0	0	0.143	0
Ach1	MTISNLLKQR	0	1	0	0	n/a	0	n/a
Pyc2	MSSSKKLAGLR	0	1	0	0	n/a	0	n/a
Rps0a	MSLPATFDLTPEDAQLLLAANTHLGAR	0	45	0	34	n/a	0	17.2
Rps1a	MAVGKNKR	0	2	0	2	n/a	0	0
Rps27a	MVLVQDLLHPTAASEAR	0	2	0	3	n/a	0	0
Asc1	MASNEVLVLR	0	5	0	3	n/a	0	0
Vps52	MDVLKEVLSLDQDKFDQLKETSR	2	0	1	0	0	0.125	0
Snu13	MSAPNPKAFPLADAALTQQILDVVQQAANLR	0	18	0	15	n/a	0	33
Pgd1	MDSIIPAGVKLDDLQVILAKNENETR	0	1	0	0	n/a	0	0.333
Bud27	MDLLAASVESTLKNLQDKR	1	1	0	0	1	0.059	0.043
Rbg2	MGIIDKIKAIEEEMAR	0	6	0	9	n/a	0	n/a
Arc35	MLHLQPQNLLIQKTLNEAIEALR	0	1	0	0	n/a	0	0.024
Act1	MDSEVAALVIDNGSGMCKAGFAGDDAPR	1	0	0	0	0	0.037	0
Rps15	MSQAVNAKKR	0	3	0	1	n/a	0	n/a
Egd1	MPIDQEKLAKLQKLSANNKVGGTR	0	10	0	3	n/a	0	n/a
Dyn2	MSDENKSTPIVKASDITDKLKEDILTISKDALDKYQLER	1	0	0	1	1	n/a	n/a
Scw10	MRFSNFLTVSALLTGALGAPAVR	0	1	0	0	n/a	0	0
Rps28A	MDNKTPVTLAKVIKVLGR	7	29	3	14	4.3	0.028	0.149
Hbn1	MSAVATYLKTLTAR	0	1	0	0	n/a	0	n/a

a and b denote PSM counts of Nt-formylated proteins from the MS/MS database search engines MS-GF+ and Comet, respectively.
c denotes relative quantification of each protein (as listed in row), based on PSM, between species as designated in each column.
*n/a, calculation of a relative ratio is not applicable, because denominator peptides were not detected.

Table S2. fMet-containing N-terminal peptides, identified using SILAC/N-terminome analysis with stationary-phase wild-type (L, Light) versus *psh1*Δ (H, Heavy) *S. cerevisiae* (see the main text and Materials and methods).

Protein	fMet-containing peptides	WT (L)[a]	*psh1Δ* (H)[a]	ratio[b] (H/L)	ratio[b] fMet/non-fMet (WT)	ratio[b] fMet/Non-fMet (*psh1Δ*)
Act1	MDSEVAALVIDNGSGMCKAGFAGDDAPR	22	26	1.2	0.014	0.017
Tim9	MDALNSKEQQEFQKVVEQKQMKDFMR	1	5	5	0.004	0.021
Gpm1	MPKLVLVR	5	1	0.2	0.217	0.077
Tdh2	MVRVAINGFGR	3	2	0.7	n/a*	n/a*
Get4	MVPAESNAVQAKLAKTLQR	1	3	3	0.048	0.158
Imp2	MQKSILLTKPDGTQSNLHSIKTETPTTVEFDSEQMER	2	2	1	0.182	0.167
Lsm7	MHQQHSKSENKPQQQR	0	3	n/a*	0	0.032
Rpl29	MAKSKNHTAHNQTR	1	2	2	0.033	0.5
Rps30A	MAKVHGSLARAGKVKSQTPKVEKTEKPKKPKGR	1	1	1	n/a	n/a
Tom6	MDGMFAMPGAAAGAASPQQPKSR	1	1	1	0,.019	0.018
Pck1	MSPSKMNATVGSTSEVEQKIR	1	1	1	n/a	n/a
Fba1	MGVEQILKR	0	2	n/a	0	0.118
Opi10	MFAAIASGNPLQLSVEVPNSNGLQHTIVLSR	1	1	1	0.25	0.25
Rpl24a	MKVEIDSFSGAKIYPGR	0	1	n/a	n/a	0.004
Ubc4	MSSSKRIAKELSDLER	0	1	n/a	n/a	n/a
Zuo1	MFSLPTLTSDITVEVNSSATKTPFVR	0	1	n/a	0	1
Rps28a	MDNKTPVTLAKVIKVLGR	0	1	n/a	0	0.006
Gpi15	MISKEYEFGKTSILNR	0	1	n/a	n/a	n/a
Fmp52	MNGLVLGATGLCGGGFLR	1	0	0	0.26	0
Pfd1	MSQIAQEMTVSLR	0	1	n/a	n/a	n/a
Cox12	MADQENSPLHTVGFDAR	1	0	0	0.5	0
Sah1	MSAPAQNYKIADISLAAFGR	0	1	n/a	n/a	n/a
Rps22a	MTRSSVLADALNAINNAEKTGKR	0	1	n/a	0	1
Fes1	MEKLLQWSIANSQGDKEAMAR	0	1	n/a	0	0.017
Yjl068c	MKVVKEFSVCGGR	1	0	0	0.091	0
Rps10b	MLMPKQER	1	0	0	0.01	0
Sec17	MSDPVELLKR	1	0	0	n/a	n/a
Smc6	MISTTISGKRPIEQVDDELLSLTAQQENEEQQQQR	0	1	n/a	n/a	1

Rps14b	MANDLVQARDNSQVFGVAR	0	1	n/a	n/a	n/a
Vac14	MEKSIAKGLSDKLYEKR	1	0	0	0.043	0
Nbl1	MIPALTPEER	1	0	0	0.167	0
Ses1	MLDINQFIEDKGGNPELIR	0	1	n/a	0	0.006
Pin4	METSSFENAPPAAINDAQDNNINTETNDQETNQQSIETR	0	1	n/a	0	0.1
Ykl151c	MLAELSHR	1	0	0	0.04	0
Ypl199c	MKGTGGVVVGTQNPVR	1	0	0	0.067	0
Uso1	MDIIQGLIQQPKIQSVDETIPTLCDRVENSTLISDRR	1	0	0	0.033	0

a denotes PSM counts of Nt-formylated proteins from stationary-phase wild-type and *psh1*Δ *S. cerevisiae*, respectively.
b denotes relative quantification of each protein (as listed in row), based on PSM, between species as designated in each column.
*n/a, calculation of a relative ratio is not applicable, because denominator peptides were not detected.

Table S3. *S. cerevisiae* strains used in this study.

Strains	Relevant genotypes	Sources
JD52	*MATa trp1-63 ura3-52 his3-200 leu2-3,112 lys2-801*	Lab collection
JD53	*MATα trp1-63 ura3-52 his3-200 leu2-3,112 lys2-801*	Lab collection
BY4741	*MATa his3-1 leu2-0 ura3-0 met15-0*	Lab collection
W303-1A	*MATa ade2-1 can1-100 his3-11,14 leu2-3,112 trp1-1 ura3-1*	Lab collection
CHY153	*arg4Δ::kanMX6* in JD52	This study
CHY367	*naa20Δ::natMX4* in JD53	This study
CHY516	*ubc8Δ::kanMX4* in BY4741	Lab collection
MGG15	*MATa his3-1 ura3-52 cdc34-2*	Lab collection
CHY909	*fmt1Δ::kanMX6* in W303-1A	This study
CHY3129	*naa20Δ::natMX4 ubr1Δ::kanMX6* in JD53	This study
CHY3174	*psh1Δ::hphMX4* in JD53	This study
CHY3176	*psh1Δ::hphMX4 naa20Δ::natMX4 ubr1Δ::kanMX6* in JD53	This study
CHY3188	*arg4Δ::kanMX6* in JD53	This study
CHY3189	*arg4Δ::kanMX6 psh1Δ::hphMX4* in JD53	This study
CHY3186	*ubr1Δ::kanMX6* in JD53	This study
CHY3196	*fmt1Δ::kanMX6* in JD53	This study
CHY3200	*gcn2Δ::natMX4* in JD53	This study
CHY3201	*gcn2Δ::natMX4 psh1Δ::hphMX4* in JD53	This study
CHY3220	*pdr5Δ::kanMX4* in BY4741	Lab collection
CHY3286	*cox5aΔ::kanMX4* in BY4741	Lab collection
CHY3323	*atp11Δ::kanMX4* in BY4741	Lab collection
CHY3328	*coq5Δ::kanMX4* in BY4741	Lab collection
CHY3330	*ufo1Δ::kanMX4* in BY4741	Lab collection
CHY3331	*ubr2Δ::kanMX4* in BY4741	Lab collection
CHY3332	*vps8Δ::kanMX4* in BY4741	Lab collection
CHY3333	*hrt3Δ::kanMX4* in BY4741	Lab collection

CHY3334	*pep5Δ::kanMX4* in BY4741	Lab collection
CHY3335	*pex12Δ::kanMX4* in BY4741	Lab collection
CHY3336	*rkr1Δ::kanMX4* in BY4741	Lab collection
CHY3337	*psh1Δ::kanMX4* in BY4741	Lab collection
CHY3338	*dia2Δ::kanMX4* in BY4741	Lab collection
CHY3339	*hrd1Δ::kanMX4* in BY4741	Lab collection
CHY3340	*siz1Δ::kanMX4* in BY4741	Lab collection
CHY3341	*ydr131cΔ::kanMX4* in BY4741	Lab collection
CHY3342	*san1Δ::kanMX4* in BY4741	Lab collection
CHY3343	*ubr1Δ::kanMX4* in BY4741	Lab collection
CHY3344	*dma1Δ::kanMX4* in BY4741	Lab collection
CHY3345	*nfi1Δ::kanMX4* in BY4741	Lab collection
CHY3346	*uls1Δ::kanMX4* in BY4741	Lab collection
CHY3347	*ylr224wΔ::kanMX4* in BY4741	Lab collection
CHY3348	*dsc3Δ::kanMX4* in BY4741	Lab collection
CHY3349	*ufd4Δ::kanMX4* in BY4741	Lab collection
CHY3350	*tul1Δ::kanMX4* in BY4741	Lab collection
CHY3351	*pex2Δ::kanMX4* in BY4741	Lab collection
CHY3352	*mdm30Δ::kanMX4* in BY4741	Lab collection
CHY3353	*mms22Δ::kanMX4* in BY4741	Lab collection
CHY3354	*far1Δ::kanMX4* in BY4741	Lab collection
CHY3355	*das1Δ::kanMX4* in BY4741	Lab collection
CHY3356	*irc20Δ::kanMX4* in BY4741	Lab collection
CHY3357	*mms1Δ::kanMX4* in BY4741	Lab collection
CHY3358	*swm1Δ::kanMX4* in BY4741	Lab collection
CHY3359	*pex10Δ::kanMX4* in BY4741	Lab collection
CHY3360	*asi2Δ::kanMX4* in BY4741	Lab collection
CHY3361	*pib1Δ::kanMX4* in BY4741	Lab collection
CHY3362	*hel1Δ::kanMX4* in BY4741	Lab collection

CHY3363	*saf1Δ::kanMX4* in BY4741	Lab collection
CHY3364	*tom1Δ::kanMX4* in BY4741	Lab collection
CHY3365	*slx5Δ::kanMX4* in BY4741	Lab collection
CHY3366	*ssm4Δ::kanMX4* in BY4741	Lab collection
CHY3367	*rad16Δ::kanMX4* in BY4741	Lab collection
CHY3368	*snt2Δ::kanMX4* in BY4741	Lab collection
CHY3369	*hul5Δ::kanMX4* in BY4741	Lab collection
CHY3370	*bre1Δ::kanMX4* in BY4741	Lab collection
CHY3371	*slx8Δ::kanMX4* in BY4741	Lab collection
CHY3372	*bul2Δ::kanMX4* in BY4741	Lab collection
CHY3373	*grr1Δ::kanMX4* in BY4741	Lab collection
CHY3374	*ylr352wΔ::kanMX4* in BY4741	Lab collection
CHY3375	*mfb1Δ::kanMX4* in BY4741	Lab collection
CHY3376	*cul3Δ::kanMX4* in BY4741	Lab collection
CHY3377	*rcy1Δ::kanMX4* in BY4741	Lab collection
CHY3378	*yhl010cΔ::kanMX4* in BY4741	Lab collection
CHY3379	*ydr132cΔ::kanMX4* in BY4741	Lab collection
CHY3380	*ste5Δ::kanMX4* in BY4741	Lab collection
CHY3381	*cos111Δ::kanMX4* in BY4741	Lab collection
CHY3382	*skp2Δ::kanMX4* in BY4741	Lab collection
CHY3383	*ymr258cΔ::kanMX4* in BY4741	Lab collection
CHY3384	*ylr108cΔ::kanMX4* in BY4741	Lab collection
CHY3385	*amn1Δ::kanMX4* in BY4741	Lab collection
CHY3386	*ybr062cΔ::kanMX4* in BY4741	Lab collection
CHY3387	*fap1Δ::kanMX4* in BY4741	Lab collection
CHY3388	*itt1Δ::kanMX4* in BY4741	Lab collection
CHY3389	*rad7Δ::kanMX4* in BY4741	Lab collection
CHY3390	*mms1Δ::kanMX4* in BY4741	Lab collection
CHY3391	*yil001wΔ::kanMX4* in BY4741	Lab collection

CHY3392	*ydr306cΔ::kanMX4* in BY4741	Lab collection
CHY3393	*cdh1Δ::kanMX4* in BY4741	Lab collection
CHY3394	*ela1Δ::kanMX4* in BY4741	Lab collection
CHY3395	*elc1Δ::kanMX4* in BY4741	Lab collection
CHY3396	*mad5Δ::kanMX4* in BY4741	Lab collection
CHY3397	*rtt101Δ::kanMX4* in BY4741	Lab collection
CHY3398	*rtc1Δ::kanMX4* in BY4741	Lab collection
CHY3399	*asr1Δ::kanMX4* in BY4741	Lab collection
CHY3400	*rad5Δ::kanMX4* in BY4741	Lab collection
CHY3401	*mag2Δ::kanMX4* in BY4741	Lab collection
CHY3402	*hul4Δ::kanMX4* in BY4741	Lab collection
CHY3403	*rad18Δ::kanMX4* in BY4741	Lab collection
CHY3404	*ufd2Δ::kanMX4* in BY4741	Lab collection
CHY3405	*asi3Δ::kanMX4* in BY4741	Lab collection
CHY3406	*dma2Δ::kanMX4* in BY4741	Lab collection
CHY3407	*asi1Δ::kanMX4* in BY4741	Lab collection

Table S4. Plasmids used in this study.

Plasmids	Descriptions	Sources
pRS314	CEN-based vector with a *TRP1* marker	Lab collection
pRS316	CEN-based vector with a *URA3* marker	Lab collection
pRS425	2μ-based vector with a *LEU2* marker	Lab collection
p425GAL	P_{GAL1}-T_{CYC1} in pRS425	Lab collection
YEplac181	2μ-based vector with a *LEU2* marker	Lab collection
pBJ1376	pBS-3xEGFP-TRP1	(*48*)
pCH178	P_{CUP1}-Ub^{R48}-CK-e^{K}-ha-Ura3 in pRS314	(*9*)
pCH1220	$P_{GAL1,10}$ in pRS424	Lab collection
pCH2167	P_{TDH3}-*Ec*FMT-T_{CYC1} in pRS316	This study
pCH2168	P_{TDH3}-*Ec*FMT^{R43L}-T_{CYC1} in pRS316	This study
pCH2182	MD-$D2^{3-11}$-GST in pET23a	This study
pCH2194	P_{FMT1}-Fmt1-3xEGFP in pRS316	This study
pCH2195	P_{FMT1}-$Fmt1^{\Delta1-26}$-3xEGFP in pRS316	This study
pCH2199	P_{CUP1}-MD-$D2^{3-11}$-GST-T_{ADH1} and P_{TDH3}-*Ec*FMT-T_{CYC1} in pRS316	This study
pCH2200	P_{CUP1}-MD-$D2^{3-11}$-GST-T_{ADH1} and P_{TDH3}-T_{CYC1} in pRS316	This study
pCH2201	P_{CUP1}-MD-$D2^{3-11}$-GST-T_{ADH1} and P_{TDH3}-*Sc*$Fmt1_{flag}$-T_{CYC1} in pRS316	This study
pCH2202	P_{CUP1}-MD-$D2^{3-11}$-GST-T_{ADH1} and P_{TDH3}-*Sc*$Fmt1^{\Delta1-26}{}_{flag}$-$T_{CYC1}$ in pRS316	This study
pCH3082	P_{GAL1}-*Ec*FMT-T_{CYC1} in pRS425	This study
pCH3083	P_{GAL1}-*Ec*FMT^{R43L}-T_{CYC1} in pRS425	This study
pCH3086	P_{CUP1}-MD-$D2^{3-11}$-e^{K}-ha-Ura3 in pRS314	This study
pCH3108	$P_{GAL1,10}$-*Ec*FMT and *Ec*PDF in pRS425	This study
pCH3109	$P_{GAL1,10}$-*Ec*FMT and *Ec*PDF^{E134A} in pRS425	This study
pCH3139	An intermediate vector with GST-T_{ADH1} in pRS314	This study
pCH3142	P_{CUP1}-MD-$D2^{3-11}$-e^{K}-ha-GST-T_{ADH1} in pRS314	This study
pCH3194	P_{CUP1}-MD-$D2^{3-11}$-e^{K}-ha-GST-T_{ADH1} and P_{ADH1}-*Ec*FMT-T_{CYC1} in pRS314	This study
pCH3196	P_{CUP1}-MD-$D2^{3-11}$-e^{K}-ha-GST-T_{ADH1} and P_{ADH1}-*Ec*FMT^{R43L}-T_{CYC1} in pRS314	This study
pCH3198	P_{CUP1}-MD-$D2^{3-11}$-e^{K}-ha-GST-T_{ADH1} and P_{TEF1}-*Ec*FMT-T_{CYC1} in pRS314	This study

pCH3200	P_{CUP1}-MD-D2$^{3-11}$-e^{K}-ha-GST-T_{ADH1} and P_{TEF1}-*Ec*FMT^{R43L}-T_{CYC1} in pRS314	This study
pCH3202	P_{CUP1}-MD-D2$^{3-11}$-e^{K}-ha-GST-T_{ADH1} and P_{TDH3}-*Ec*FMT-T_{CYC1} in pRS314	This study
pCH3204	P_{CUP1}-MD-D2$^{3-11}$-e^{K}-ha-GST-T_{ADH1} and P_{TDH3}-*Ec*FMT^{R43L}-T_{CYC1} in pRS314	This study
pCH3206	P_{CUP1}-Ub^{R48}-MD-D2$^{3-11}$-e^{K}-ha-Ura3 in pRS314	This study
pCH3219	P_{CUP1}-MD-D2$^{3-11}$-e^{K}-ha-GST-T_{ADH1} and P_{ADH1}-*Ec*FMT-T_{CYC1} in pRS316	This study
pCH3220	P_{CUP1}-MD-D2$^{3-11}$-e^{K}-ha-GST-T_{ADH1} and P_{ADH1}-*Ec*FMT^{R43L}-T_{CYC1} in pRS316	This study
pCH3225	P_{CUP1}-MD-D2$^{3-11}$-e^{K}-ha-GST-T_{ADH1} and P_{ADH1}-T_{CYC1} in pRS314	This study
pCH3226	P_{CUP1}-MD-D2$^{3-11}$-e^{K}-ha-GST-T_{ADH1} and P_{TDH3}-T_{CYC1} in pRS314	This study
pCH3227	P_{CUP1}-MD-D2$^{3-11}$-e^{K}-ha-GFP-T_{ADH1} and P_{ADH1}-*Ec*FMT-T_{CYC1} in pRS314	This study
pCH3228	P_{CUP1}-MD-D2$^{3-11}$-e^{K}-ha-GFP-T_{ADH1} and P_{ADH1}-*Ec*FMT^{R43L}-T_{CYC1} in pRS314	This study
pCH3245	P_{CUP1}-MD-D2$^{3-11}$-e^{K}-ha-GST-T_{ADH1} and P_{TDH3}-*Ec*FMT-T_{CYC1} in pRS316	This study
pCH3246	P_{CUP1}-MD-D2$^{3-11}$-e^{K}-ha-GST-T_{ADH1} and P_{TDH3}-T_{CYC1} in pRS316	This study
pCH3282	P_{TDH3}-Psh1$_{flag}$-T_{CYC1} in YEplac181	This study
pCH3293	P_{CUP1}-MD-D2$^{3-11}$-e^{K}-ha-GST-T_{ADH1} and P_{ADH1}-T_{CYC1} in pRS314	This study
pCH3323	P_{ADH1}-*Ec*FMT-T_{CYC1} in pRS316	This study
pCH3324	P_{ADH1}-*Ec*FMT^{R43L}-T_{CYC1} in pRS316	This study
pCH3383	P_{TDH3}-mito-mCherry-T_{CYC1} in pRS314	This study
pCH3397	P_{ADH1}-*Ec*PDF-T_{TEF1} in pRS425	This study
pCH3398	P_{ADH1}-*Ec*PDF^{E134A}-T_{TEF1} in pRS425	This study
pCH3401	P_{CUP1}-Rps22a$_{ha}$-T_{ADH1} and P_{ADH1}-T_{CYC1} in pRS314	This study
pCH3402	P_{CUP1}-Pgd1$_{ha}$-T_{ADH1} and P_{ADH1}-T_{CYC1} in pRS314	This study
pCH3417	P_{CUP1}-MD-D2$^{3-11}$-GST-T_{ADH1} and P_{TDH3}-*Sc*Fmt1$_{myc}$-T_{CYC1} in pRS314	This study
pCH3423	P_{CYC1}-Ifm1-EGFP-T_{CYC1} in pRS316	This study
pCH3425	P_{CYC1}-Sod2-EGFP-T_{CYC1} in pRS316	This study
pCH3426	P_{CYC1}-Cit1-EGFP-T_{CYC1} in pRS316	This study
pCH3558	P_{CUP1}-Cse4$_{ha}$-T_{ADH1} and P_{ADH1}-*Ec*FMT-T_{CYC1} in pRS316	This study

pCH3561	P_{CUP1}-Cse4$_{ha}$-T_{ADH1} and P_{ADH1}-*Ec*FMT^{R43L}-T_{CYC1} in pRS316	This study
pCH3567	P_{CUP1}-Cse4$^{HFD}_{ha}$-T_{ADH1} and P_{ADH1}-*Ec*FMT-T_{CYC1} in pRS316	This study
pCH3568	P_{CUP1}-Cse4$^{HFD}_{ha}$-T_{ADH1} and P_{ADH1}-*Ec*FMT^{R43L}-T_{CYC1} in pRS316	This study
pCH3569	P_{CUP1}-Cse4$_{ha}$-T_{ADH1} and P_{ADH1}-T_{CYC1} in pRS316	This study
pCH3570	P_{CUP1}-Cse4$^{HFD}_{ha}$-T_{ADH1} and P_{ADH1}-T_{CYC1} in pRS316	This study
pCH3592	P_{CUP1}-Ub^{R48}-MD-D2$^{3-11}$-GST-T_{ADH1} and P_{TDH3}-*Ec*FMT-T_{CYC1} in pRS316	This study
pCH3626	P_{CUP1}-Rps22a$_{ha}$-T_{ADH1} and P_{ADH1}-*Ec*FMT-T_{CYC1} in pRS314	This study
pCH3646	P_{CUP1}-Rps22a$_{ha}$-T_{ADH1} and P_{ADH1}-*Ec*FMT^{R43L}-T_{CYC1} in pRS314	This study
pCH5109	P_{ADH1}-*Ec*PDF-T_{TEF1} in pRS314	This study
pCH5110	P_{ADH1}-*Ec*PDF^{E134A}-T_{TEF1} in pRS314	This study
pCH5136	P_{CUP1}-Pgd1$_{ha}$-T_{ADH1} and P_{ADH1}-*Ec*FMT-T_{CYC1} in pRS314	This study
pCH5144	P_{CUP1}-Pgd1$_{ha}$-T_{ADH1} and P_{ADH1}-*Ec*FMT^{R43L}-T_{CYC1} in pRS314	This study
pCH5152	P_{CUP1}-Hxk1$_{ha}$-T_{ADH1} and P_{ADH1}-*Ec*FMT-T_{CYC1} in pRS314	This study
pCH5153	P_{CUP1}-Hxk1$_{ha}$-T_{ADH1} and P_{ADH1}-*Ec*FMT^{R43L}-T_{CYC1} in pRS314	This study

Table S5. Some PCR primers used in this study.

Name	**Primer sequences**
OCH2125	5'-CGCGGATCCATGTCAGAATCACTACGTATT-3'
OCH2126	5'-CCGCTCGAGAGTGGACTATCAGACCAGACGGTTGCC-3'
OCH2127	5'-GCTGGGCATCAGTTTTTTACCCAGTCCTGCCGGTCGGTCTGGCTG-3'
OCH2128	5'-CAGCCAGACCGACCGGCAGGACTGGGTAAAAAACTGATGCCCAGC-3'
OCH2201	5'-AACGTCGACGGAATGTAGAGCCGGGTTACAGGA-3'
OCH2207	5'-ACTGGATCCCAGGAAAACTAACTTTTCACTCAGGG-3'
OCH2208	5'-CCGGAATTCGCAGCAAATCTGAAGGAATGT-3'
OCH2209	5'-CCCGTCGACTTGTTTGATACGCCGTTTTCA-3'
OCH2210	5'-CCCGTCGACATGGTGCAGCCCTTGAATGTGCTT-3'
OCH2228	5'-CGCAGATCTATGGTTAAAATGAGAAGAATAACA-3'
OCH2229	5'-ACTAGATCTATGGTGCAGCCCTTGAATGTGCTTTTC-3'
OCH2237	5'-GGGCATATGGACATTGCGATCGGT-3'
OCH2240	5'-GGGGAGCTCCCGGTAGAGGTG-3'
OCH3098	5'-GGGGAATTCATGGACATTGCGATCGGTACATATCA-3'
OCH3101	5'-GGGGGATCCTTTCTCTTGATATGTACCGATCGCAAT-3'
OCH3111	5'-CGCGAATTCATGTCAGTTTTGCAAGTGTTACAT-3'
OCH3112	5'-GCGGAGCTCTTAAGCCCGGGCTTTCAGACGATC-3'
OCH3113	5'- GCCATCTGTATTCAGCATGCAATGGATCACCTGGTCGGC-3'
OCH3114	5'- GCCGACCAGGTGATCCATTGCATGCTGAATACAGATGGC-3'
OCH3190	5'-ACAGGTACCGGCCGCAAATTAAAG-3'
OCH3191	5'-ATAGGGCCCGCGAATTTCTTATGATTTATG-3'
OCH3192	5'-ATAGAGCTCCCGGTAGAGGTGTGGTCAATAAG-3'
OCH3193	5'-GACACTAGTTCCCCTATACTAGGTTATTGG-3'
OCH3194	5'-ATAGGGCCCTTATTTTGGAGGATGGTCGCC-3'
OCH3195	5'-GACACTAGTTCTAAAGGTGAAGAATTATTC-3'
OCH3196	5'-ATAGGGCCCTTATTTGTACAATTCATCCATAC-3'
OCH3197	5'-ACAGTCGACAGCCGAGGCCGAGCGGCCGCCTAGTTAGAAAAAGACATTTTT G-3'
OCH3198	5'-CGCACTAGTCTGGCCAAGGAAAGCGGCGTAATC-3'
OCH3241	5'-ACAGTCGACATCCTTTTGTTGTTTCCGGG-3'
OCH3242	5'-AGACCCGGGGCGGCCAGCTTGGAGTTGAT-3'
OCH3243	5'-ACAGTCGACTCATTATCAATACTCGCCAT-3'
OCH3244	5'-AGACCCGGGATCCGTCGAAACTAAGTTCT-3'
OCH3245	5'-ACAGTCGACCATAGCTTCAAAATGTTTCT-3'
OCH3246	5'-AGACCCGGGAAACTTAGATTAGATTGCTA-3'
OCH3247	5'-ACACCCGGGACAAGATCTATGTCAGAATCACTACGTATT-3'
OCH3251	5'-CTACCGCGGTGGTATGGACATTGCGATCGGTACATATCA-3'
OCH3256	5'-ATACCCGGGGTCGAAACTAAGTTCTGGTG-3'
OCH3286	5'-AAACCCGGGATGGGCGACGAATTACACAACCG-3'

OCH3287	5'-AAACTCGAGTTACTTGTCATCATCGTCCTTGTAGTCACTAGTACC AGATTCATCGTCACTGTCTCCTAG-3'
OCH3326	5'- CTCACTGACTGCGGCCGCGATAATATCACCAAACATGTTGTTGGTAAT AACAACACCGATCCTTTTGTTGTTTCCGGGTGTAC-3'
OCH3327	5'- AATGGATCCGTTACAGTTTGTTTTTCTTAATATCTATTTCGCGGCCAGC TTGGAGTTGATTGTA-3'
OCH3328	5'-CATAGATCTATGTCAGTTTTGCAAGTGTTACAT-3'
OCH3331	5'- AATGTCGACTGCTCCCGGCATCCGCTTACAGACAAGCTGTGACCGTCT CCAGTATAGCGACCAGCATTCACAT-3'
OCH3386	5'-ATTACTAGTTTATTTGTACAATTCATCCATACC-3'
OCH3398	5'-TATCCCGGGATGCTCAGAAGACACGGATTATTC-3'
OCH3417	5'-TATCCCGGGATGTCAGCGATATTATCAACAACT-3'
OCH3421	5'- TATCCCGGGATGGCCTCCACTCGTGTCCTCGCCTCTCGCCTGGCCTCC CAGATGGCTGCTTCCGCCAAGGTTGCCC-3'
OCH3422	5'- AGTCTGGATGGTGCGCTTGCTGACCTGAGCAACGCGGACAGCAGGGC GGGCAACCTTGGCGGAAGCA-3'
OCH3423	5'- GCAAGCGCACCATCCAGACTGGCTCCCCCCTCCAGACCCTCAAGCGC ACCCAGATGACCTCCATCGT-3'
OCH3424	5'- TATGGATCCGGAAGAGTAGGCGCGCTTCTGGAAAGCCTGGCGGGTGG TGGCGTTGACGATGGAGGTCATCTGGGT-3'
OCH3470	5'- ATAGGATCCGGTGGATCTGGAGGTTCTATGTCTAAAGGTGAAGAATT ATTC-3'
OCH3471	5'- ATAGGATCCGGTGGATCTGGAGGTTCTATGGTGAGCAAGGGCGAGGA GGAT-3'
OCH3472	5'-TATACTAGTTTACTTGTACAGCTCGTCCATGCCGCC-3'
OCH3549	5'-GGCGAATTCATGTCAAGTAAACAACAATGG-3'
OCH3550	5'-GAAGGATCCAATAAACTGTCCCCTGATTCT-3'
OCH3586	5'-TATGGATCCTACCCATACGACGTCCCAGATTACG-3'
OCH3587	5'-AAAGAAGTTACAGACGAGTTTCAAGATTTCAAGACCGACTTG-3'
OCH3588	5'-CATTATAGTAATTCTTTTTGCGTGAATAGCAGCCAGATTAGT-3'
OCH3589	5'-GGTCTTGAAATCTTGAAACTCGTCTGTAACTTCTTT-3'
OCH3590	5'-CTGGCTGCTATTCACGCAAAAAGAATTACTATAATG-3'
OCH3651	5'-GGCGGATCCTCCCCTATACTAGGTTATTGG-3'
OCH3722	5'- AATGGATCCATGACCAGATCTTCCGTT -3'
OCH3723	5'- GCCACTAGTGTAAACGAAACCCAAAAT -3'

OCH4685	5'- ATACTGCAGGAACAAAAACTTATTTCTGAAGAAGATCTGTAACTTAA GTCATGTAATTAGTTATGTCAC-3'
OCH4686	5'-AATGGATCCGTTCTTACTTTCGATTTTCTTTAC-3'
OCH4687	5'-AATGGATCCCAAGTAACGAGGAACTCGCACGTT-3'
OCH4688	5'-AATCCCGGGATGTTCGCGAAAACAGCAGCTGCT-3'
OCH4689	5'-AATGGATCCGATCTTGCCAGCATCGAATCTTCT-3'
OCH5166	5'- ACAGTCGACAGCCGAGGCCGAGCGGCCGCGATAATATCACCAAACAT GTTGTTGGTAATAACAACACCGCTCATTTGGCGAGCGTTGGT-3'
OCH5167	5'- TATGAATTCGTTACAGTTTGTTTTTCTTAATATCTATTTCTTAGTGTGT GTATTTGTGTTTG-3'
OCH5178	5'-AATGGATCCATGGTTCATTTAGGTCCAAAGAAA-3'
OCH5179	5'-AATACTAGTAGCGCCAATGATACCAAGAGACTT-3'
OCH5182	5'-AATAGATCTATGGACTCGATTATACCGGCAGGC-3'
OCH5183	5’-AATACTAGTCAAGAAATCCATGTTCAGACCACC-3’
OCH6565	5'-ATAGAGCTCCCGGTAGAGGTGTGGTCAATAAG-3'

References and Notes

1. B. S. Laursen, H. P. Sørensen, K. K. Mortensen, H. U. Sperling-Petersen, Initiation of protein synthesis in bacteria. *Microbiol. Mol. Biol. Rev.* **69**, 101–123 (2005). doi:10.1128/MMBR.69.1.101-123.2005 Medline

2. D. Mazel, S. Pochet, P. Marlière, Genetic characterization of polypeptide deformylase, a distinctive enzyme of eubacterial translation. *EMBO J.* **13**, 914–923 (1994). doi:10.1002/j.1460-2075.1994.tb06335.x Medline

3. G. Kramer, D. Boehringer, N. Ban, B. Bukau, The ribosome as a platform for co-translational processing, folding and targeting of newly synthesized proteins. *Nat. Struct. Mol. Biol.* **16**, 589–597 (2009). doi:10.1038/nsmb.1614 Medline

4. V. Ramesh, C. Köhrer, U. L. RajBhandary, Expression of *Escherichia coli* methionyl-tRNA formyltransferase in *Saccharomyces cerevisiae* leads to formylation of the cytoplasmic initiator tRNA and possibly to initiation of protein synthesis with formylmethionine. *Mol. Cell. Biol.* **22**, 5434–5442 (2002). doi:10.1128/MCB.22.15.5434-5442.2002 Medline

5. R. Bingel-Erlenmeyer, R. Kohler, G. Kramer, A. Sandikci, S. Antolić, T. Maier, C. Schaffitzel, B. Wiedmann, B. Bukau, N. Ban, A peptide deformylase-ribosome complex reveals mechanism of nascent chain processing. *Nature* **452**, 108–111 (2008). doi:10.1038/nature06683 Medline

6. C. Giglione, S. Fieulaine, T. Meinnel, N-terminal protein modifications: Bringing back into play the ribosome. *Biochimie* **114**, 134–146 (2015). doi:10.1016/j.biochi.2014.11.008 Medline

7. K. I. Piatkov, T. T. M. H. Vu, C.-S. Hwang, A. Varshavsky, Formyl-methionine as a degradation signal at the N-termini of bacterial proteins. *Microb. Cell* **2**, 376–393 (2015). doi:10.15698/mic2015.10.231 Medline

8. H. Aksnes, A. Drazic, M. Marie, T. Arnesen, First things first: Vital protein marks by N-terminal acetyltransferases. *Trends Biochem. Sci.* **41**, 746–760 (2016). doi:10.1016/j.tibs.2016.07.005 Medline

9. C. S. Hwang, A. Shemorry, A. Varshavsky, N-terminal acetylation of cellular proteins creates specific degradation signals. *Science* **327**, 973–977 (2010). doi:10.1126/science.1183147 Medline

10. A. Varshavsky, The N-end rule pathway and regulation by proteolysis. *Protein Sci.* **20**, 1298–1345 (2011). doi:10.1002/pro.666 Medline

11. A. Shemorry, C. S. Hwang, A. Varshavsky, Control of protein quality and stoichiometries by N-terminal acetylation and the N-end rule pathway. *Mol. Cell* **50**, 540–551 (2013). doi:10.1016/j.molcel.2013.03.018 Medline

12. H. K. Kim, R.-R. Kim, J.-H. Oh, H. Cho, A. Varshavsky, C.-S. Hwang, The N-terminal methionine of cellular proteins as a degradation signal. *Cell* **156**, 158–169 (2014). doi:10.1016/j.cell.2013.11.031 Medline

13. S. E. Park, J.-M. Kim, O.-H. Seok, H. Cho, B. Wadas, S.-Y. Kim, A. Varshavsky, C.-S. Hwang, Control of mammalian G protein signaling by N-terminal acetylation and the N-

end rule pathway. *Science* **347**, 1249–1252 (2015). doi:10.1126/science.aaa3844 Medline

14. A. Bachmair, D. Finley, A. Varshavsky, In vivo half-life of a protein is a function of its amino-terminal residue. *Science* **234**, 179–186 (1986). doi:10.1126/science.3018930 Medline

15. T. Tasaki, S. M. Sriram, K. S. Park, Y. T. Kwon, The N-end rule pathway. *Annu. Rev. Biochem.* **81**, 261–289 (2012). doi:10.1146/annurev-biochem-051710-093308 Medline

16. D. Finley, H. D. Ulrich, T. Sommer, P. Kaiser, The ubiquitin-proteasome system of *Saccharomyces cerevisiae*. *Genetics* **192**, 319–360 (2012). doi:10.1534/genetics.112.140467 Medline

17. R. Schmidt, R. Zahn, B. Bukau, A. Mogk, ClpS is the recognition component for *Escherichia coli* substrates of the N-end rule degradation pathway. *Mol. Microbiol.* **72**, 506–517 (2009). doi:10.1111/j.1365-2958.2009.06666.x Medline

18. D. J. Gibbs, J. Bacardit, A. Bachmair, M. J. Holdsworth, The eukaryotic N-end rule pathway: Conserved mechanisms and diverse functions. *Trends Cell Biol.* **24**, 603–611 (2014). doi:10.1016/j.tcb.2014.05.001 Medline

19. N. Dissmeyer, S. Rivas, E. Graciet, Life and death of proteins after protease cleavage: Protein degradation by the N-end rule pathway. *New Phytol.* **218**, 929–935 (2018). doi:10.1111/nph.14619 Medline

20. S. J. Chen, X. Wu, B. Wadas, J.-H. Oh, A. Varshavsky, An N-end rule pathway that recognizes proline and destroys gluconeogenic enzymes. *Science* **355**, eaal3655 (2017). doi:10.1126/science.aal3655 Medline

21. I. Rivera-Rivera, G. Román-Hernández, R. T. Sauer, T. A. Baker, Remodeling of a delivery complex allows ClpS-mediated degradation of N-degron substrates. *Proc. Natl. Acad. Sci. U.S.A.* **111**, E3853–E3859 (2014). doi:10.1073/pnas.1414933111 Medline

22. S. M. Shim, H. R. Choi, K. W. Sung, Y. J. Lee, S. T. Kim, D. Kim, S. R. Mun, J. Hwang, H. Cha-Molstad, A. Ciechanover, B. Y. Kim, Y. T. Kwon, The endoplasmic reticulum-residing chaperone BiP is short-lived and metabolized through N-terminal arginylation. *Sci. Signal.* **11**, eaan0630 (2018). doi:10.1126/scisignal.aan0630 Medline

23. J. H. Oh, J. Y. Hyun, A. Varshavsky, Control of Hsp90 chaperone and its clients by N-terminal acetylation and the N-end rule pathway. *Proc. Natl. Acad. Sci. U.S.A.* **114**, E4370–E4379 (2017). doi:10.1073/pnas.1705898114 Medline

24. K. I. Piatkov, C. S. Brower, A. Varshavsky, The N-end rule pathway counteracts cell death by destroying proapoptotic protein fragments. *Proc. Natl. Acad. Sci. U.S.A.* **109**, E1839–E1847 (2012). doi:10.1073/pnas.1207786109 Medline

25. B. Wadas, K. I. Piatkov, C. S. Brower, A. Varshavsky, Analyzing N-terminal arginylation through the use of peptide arrays and degradation assays. *J. Biol. Chem.* **291**, 20976–20992 (2016). doi:10.1074/jbc.M116.747956 Medline

26. R.-G. Hu, J. Sheng, X. Qi, Z. Xu, T. T. Takahashi, A. Varshavsky, The N-end rule pathway as a nitric oxide sensor controlling the levels of multiple regulators. *Nature* **437**, 981–986 (2005). doi:10.1038/nature04027 Medline

27. D. C. Scott, J. K. Monda, E. J. Bennett, J. W. Harper, B. A. Schulman, N-terminal acetylation acts as an avidity enhancer within an interconnected multiprotein complex. *Science* **334**, 674–678 (2011). doi:10.1126/science.1209307 Medline

28. C.-S. Hwang, A. Shemorry, D. Auerbach, A. Varshavsky, The N-end rule pathway is mediated by a complex of the RING-type Ubr1 and HECT-type Ufd4 ubiquitin ligases. *Nat. Cell Biol.* **12**, 1177–1185 (2010). doi:10.1038/ncb2121 Medline

29. W. S. Choi, B.-C. Jeong, Y. J. Joo, M.-R. Lee, J. Kim, M. J. Eck, H. K. Song, Structural basis for the recognition of N-end rule substrates by the UBR box of ubiquitin ligases. *Nat. Struct. Mol. Biol.* **17**, 1175–1181 (2010). doi:10.1038/nsmb.1907 Medline

30. E. Matta-Camacho, G. Kozlov, F. F. Li, K. Gehring, Structural basis of substrate recognition and specificity in the N-end rule pathway. *Nat. Struct. Mol. Biol.* **17**, 1182–1187 (2010). doi:10.1038/nsmb.1894 Medline

31. M. K. Kim, S. J. Oh, B. G. Lee, H. K. Song, Structural basis for dual specificity of yeast N-terminal amidase in the N-end rule pathway. *Proc. Natl. Acad. Sci. U.S.A.* **113**, 12438–12443 (2016). doi:10.1073/pnas.1612620113 Medline

32. A. Varshavsky, 'Spalog' and 'sequelog': Neutral terms for spatial and sequence similarity. *Curr. Biol.* **14**, R181–R183 (2004). doi:10.1016/j.cub.2004.02.014 Medline

33. G. Hewawasam, M. Shivaraju, M. Mattingly, S. Venkatesh, S. Martin-Brown, L. Florens, J. L. Workman, J. L. Gerton, Psh1 is an E3 ubiquitin ligase that targets the centromeric histone variant Cse4. *Mol. Cell* **40**, 444–454 (2010). doi:10.1016/j.molcel.2010.10.014 Medline

34. P. Ranjitkar, M. O. Press, X. Yi, R. Baker, M. J. MacCoss, S. Biggins, An E3 ubiquitin ligase prevents ectopic localization of the centromeric histone H3 variant via the centromere targeting domain. *Mol. Cell* **40**, 455–464 (2010). doi:10.1016/j.molcel.2010.09.025 Medline

35. W. C. Au, A. R. Dawson, D. W. Rawson, S. B. Taylor, R. E. Baker, M. A. Basrai, A novel role of the N terminus of budding yeast histone H3 variant Cse4 in ubiquitin-mediated proteolysis. *Genetics* **194**, 513–518 (2013). doi:10.1534/genetics.113.149898 Medline

36. M. B. Metzger, J. L. Scales, M. F. Dunklebarger, A. M. Weissman, The ubiquitin ligase (E3) Psh1p is required for proper segregation of both centromeric and two-micron plasmids in *Saccharomyces cerevisiae*. *G3 (Bethesda)* **7**, 3731–3743 (2017). Medline

37. H. Cheng, X. Bao, X. Gan, S. Luo, H. Rao, Multiple E3s promote the degradation of histone H3 variant Cse4. *Sci. Rep.* **7**, 8565 (2017). doi:10.1038/s41598-017-08923-w Medline

38. P. J. Robinson, M. J. Trnka, D. A. Bushnell, R. E. Davis, P.-J. Mattei, A. L. Burlingame, R. D. Kornberg, Structure of a complete mediator-RNA polymerase II pre-initiation complex. *Cell* **166**, 1411–1422.e16 (2016). doi:10.1016/j.cell.2016.08.050 Medline

39. F. M. Ausubel, R. Brent, R. E. Kingston, D. D. Moore, J. G. Seidman, J. A. Smith, D. Struhl, Eds., *Current Protocols in Molecular Biology* (Wiley, 2010).40. F. Sherman, Getting started with yeast. *Methods Enzymol.* **194**, 3–21 (1991). doi:10.1016/0076-6879(91)94004-V Medline

41. M. S. Longtine, A. McKenzie 3rd, D. J. Demarini, N. G. Shah, A. Wach, A. Brachat, P.

Philippsen, J. R. Pringle, Additional modules for versatile and economical PCR-based gene deletion and modification in *Saccharomyces cerevisiae*. *Yeast* **14**, 953–961 (1998). doi:10.1002/(SICI)1097-0061(199807)14:10<953:AID-YEA293>3.0.CO;2-U Medline

42. C. Janke, M. M. Magiera, N. Rathfelder, C. Taxis, S. Reber, H. Maekawa, A. Moreno-Borchart, G. Doenges, E. Schwob, E. Schiebel, M. Knop, A versatile toolbox for PCR-based tagging of yeast genes: New fluorescent proteins, more markers and promoter substitution cassettes. *Yeast* **21**, 947–962 (2004). doi:10.1002/yea.1142 Medline

43. S. Spector, J. M. Flynn, B. Tidor, T. A. Baker, R. T. Sauer, Expression of N-formylated proteins in *Escherichia coli*. *Protein Expr. Purif.* **32**, 317–322 (2003). doi:10.1016/j.pep.2003.08.004 Medline

44. J. Cox, M. Mann, MaxQuant enables high peptide identification rates, individualized p.p.b.-range mass accuracies and proteome-wide protein quantification. *Nat. Biotechnol.* **26**, 1367–1372 (2008). doi:10.1038/nbt.1511 Medline

45. J. Yeom, S. Ju, Y. Choi, E. Paek, C. Lee, Comprehensive analysis of human protein N-termini enables assessment of various protein forms. *Sci. Rep.* **7**, 6599 (2017). doi:10.1038/s41598-017-06314-9 Medline

46. B. Westermann, W. Neupert, Mitochondria-targeted green fluorescent proteins: Convenient tools for the study of organelle biogenesis in *Saccharomyces cerevisiae*. *Yeast* **16**, 1421–1427 (2000). doi:10.1002/1097-0061(200011)16:15<1421:AID-YEA624>3.0.CO;2-U Medline

47. L. Vial, P. Gomez, M. Panvert, E. Schmitt, S. Blanquet, Y. Mechulam, Mitochondrial methionyl-tRNAfMet formyltransferase from *Saccharomyces cerevisiae*: Gene disruption and tRNA substrate specificity. *Biochemistry* **42**, 932–939 (2003). doi:10.1021/bi026901x Medline

48. W. L. Lee, J. R. Oberle, J. A. Cooper, The role of the lissencephaly protein Pac1 during nuclear migration in budding yeast. *J. Cell Biol.* **160**, 355–364 (2003). doi:10.1083/jcb.200209022 Medline